1

Higgs working group report

Conveners: Sally Dawson (BNL), Andrei Gritsan (Johns Hopkins), Heather Logan (Carleton),
Jianming Qian (Michigan), Chris Tully (Princeton), Rick Van Kooten (Indiana)
Draft of August 6, 2013

1.1 Introduction

The quest to understand the origin of mass spans at least four major energy frontier facilities in the last 25 years – from the SLC linear e^+e^- collider at SLAC and LEP circular e^+e^- collider at CERN, to the Tevatron proton-antiproton collider at Fermilab, and finally to the LHC at CERN. Now, for the first time, Higgs physics is experimentally verified to be an inextricable part of the universe and the physical laws that govern it. While we do not know at this time whether the simplest possible incarnation of the Higgs mechanism is what occurs in Nature, the fact that the new boson was discovered in the search for the Standard Model Higgs boson indicates that the basic features of the Higgs mechanism are correct. Any significant deviation in the properties or couplings of the Higgs boson imply fundamental changes to the understanding of elementary particles and interactions. Furthermore, the role of the Higgs field in early universe physics and in the unification of the forces of Nature are highly sensitive to Higgs boson properties including the mass, total width, spin, couplings, CP mixtures, and the existence of multiple Higgs bosons. With this perspective, the future of the energy frontier is contemplated with a focus on precision measurements of high statistics samples of Higgs bosons produced in ideal conditions for laboratory studies.

The compilation of the Higgs Snowmass Report is based on input in the form of White Papers from the particle physics community. All major precision Higgs physics projects with substantial representation in the US particle physics and accelerator physics communities have been included in this report. These communities are listed here (in alphabetical order):

- Compact Linear Collider (CLIC) [1]
- Gamma-Gamma Collider
- International Linear Collider (ILC) [2, 3]
- Large Hadron Collider High Luminosity Upgrade (HL-LHC)
- Muon Collider (μC)
- Triple-Large Electron-Positron Collider (TLEP) [4]

The proposed running periods and integrated luminosities at each of the center-of-mass energies for the above facilities are listed in Table 1-1.

The report has two primary goals. The first is to identify the key elements of a precision Higgs program and the fundamental importance of this science as a human endeavor to understand the universe and the laws

Table 1-1. *Proposed running periods and integrated luminosities at each of the center-of-mass energies for each facility.*

Facility	HL-LHC	ILC	ILC(LumiUp)	CLIC	TLEP (4 IPs)	HE-LHC	VLHC
$\sqrt{s}$ (GeV)	14,000	250/500/1000	250/500/1000	350/1400/3000	240/350	33,000	100,000
$\int \mathcal{L}dt$ (fb^{-1})	3000/expt	250+500+1000	1150+1600+2500	500+1500+2000	10,000+2600	3000	3000
$\int dt$ (10^7s)	6	3+3+3	(ILC 3+3+3) + 3+3+3	3.1+4+3.3	5+5	6	6

of physics. The second is to document the precision and physics potential presented during Snowmass for the above listed community initiatives to develop precision Higgs programs. This report does not judge the status, maturity, feasibility, or readiness of any of these initiatives. The reader should refer to the report of the Frontier Capabilities Group for this information. The report will also identify unique strengths of different collider initiatives and detector concepts and their importance to the precision Higgs program. The detailed charge to the Higgs Snowmass committee is listed below.

1.1.1 Charge to the Higgs Snowmass Committee

1. Provide a compact summary of the measurements on and searches for the SM Higgs boson, including information from LEP, the Tevatron, and the LHC. Include in this summary a survey of searches for non-minimal Higgs sectors.
2. Provide a compact summary of the theoretical motivations to explore the properties of the Higgs boson to high precision.
    a) What is the full phenomenological profile of the Higgs boson? What are the predicted production modes, the final states, and the experimental observables?
    b) What are the ranges of predictions for deviations from Standard Model properties that enter from new physics? Which production and decay channels and boson properties are most sensitive to these deviations?
    c) What can be learned from the discovery of bosons from non-minimal Higgs sectors? What is the phenomenology of non-minimal Higgs models?
    d) To what extent are properties of the Higgs boson and the Higgs sector in general important for understanding fundamental physics and the universe?
3. Organize a set of simulation studies to evaluate the level of precision that can be achieved on Higgs physics measurements for the range of choices of accelerator facilities and detector capabilities under consideration by the Facilities/Instrumentation groups. Include studies of search sensitivities for non-minimal Higgs sectors.
    a) To what degree can a particular experimental program ascertain whether the resonance at 126 GeV is the Standard Model Higgs boson? To what precision can each of the measured properties of the Higgs boson be determined and tested against SM predictions?
    b) What are the search sensitivities for bosons in non-minimal Higgs sectors?
    c) The studies should summarize their results in terms of these areas:
        i. Mass and width measurements;

ii. "Couplings" in terms of production cross section by process and branching fractions by decay mode, including searches for non-SM couplings;

iii. "Tensor structure" in terms of quantum numbers (J^{CP}) and effective couplings in the Lagrangian;

iv. Couplings and properties governing the Higgs potential.

d) What are intrinsic advantages of particular experimental programs? Are there unique capabilities to reconstructing particular decays or unique sensitivities to particular rare decay rates? Are there properties that can be determined in some experimental programs and not in others? To what extent can complementary programs enhance the overall Higgs physics program?

e) Provide cross-calibration for the simulation tools to provide a record of what intrinsic performances and assumptions went into these results.

1.2 Coupling Measurements

The central question about the particle discovered at 126 GeV is whether this is "The Higgs Boson" or only one degree of freedom of a bigger story. If there is more than one Higgs boson, and theories such as supersymmetry require there to be multiple bosons at the TeV scale, then the couplings of the 126 GeV boson to matter will not directly correspond to the coupling strengths predicted from the masses of the elementary particles. Additional parameters that describe the mixing of multiple Higgs boson states, or the ratio of vacuum expectation values, or in general the effects of additional degrees of freedom in the Higgs sector will result in deviations in the coupling measurements relative to Standard Model expectations. This is especially true of the loop-induced decays and production modes of the 126 GeV boson where new particles can enter the loops.

The precisions that can be obtained on the coupling measurements are projected for the LHC and e^+e^- machines. A muon collider is expected to be capable of a similar program as the e^+e^- machines, but detector simulations to extract these estimates have not been completed at this time.

Extractions of the Higgs coupling constants from measured decay modes can serve to limit various new physics models, or to confirm the validity of the Standard Model. The conclusions derived from this exercise depend on the uncertainties in the calculation of the Standard Model cross sections and branching ratios. In this subsection, we discuss the uncertainties on the theoretical predictions of the Higgs branching ratios, which have been tabulated by the LHC Higgs cross section working group [5, 6].

There are two types of uncertainties which arise when computing the uncertainties on Higgs branching ratios: parametric uncertainties and theoretical uncertainties. The parametric uncertainties describe the dependence of the predictions on the input parameters. For a 126 GeV Standard Model Higgs boson, the parametric uncertainties arise predominantly from the b mass and α_s and we use the values given in Table 1-2. The parametric uncertainties are combined in quadrature. The theoretical uncertainties are estimated from the QCD scale dependence and from higher order electroweak interactions and are listed in Table 1-3. The errors on the predictions for the branching ratios for a 126 GeV Standard Model Higgs boson are given in Table 1-4. The uncertainties on the total widths are given in Table 1-5, where the parametric errors from $\Delta\alpha_s$, Δm_b, Δm_c and the theory uncertainties are given separately. The dominant source of the electroweak uncertainty is from NLO corrections which are not included exactly in the study. These electroweak uncertainties can be expected to be reduced in the future. It is also possible that the uncertainty on the b quark mass may be reduced by future lattice calculations, as shown in Table 1-6. We note that a reduction in the uncertainty in m_b by a factor of 2 will reduce the uncertainty on the width $H \to b\bar{b}$ from 6% to $\sim 5\%$.

Table 1-2. *Parametric uncertainties used by the Higgs Cross Section Working group to determine Higgs branching ratio and width uncertainties [5, 7].*

Parameter	Central Value	Uncertainty
$\alpha_s(M_Z)$	0.119	± 0.002(90% CL)
m_c	1.42 GeV	± 0.03 GeV
m_b	4.49 GeV	± 0.06 GeV
m_t	172.5 GeV	± 2.5 GeV

Table 1-3. *Theory Uncertainties for $M_H = 126$ GeV Higgs branching ratio determination [7, 6].*

Decay	QCD Uncertainty	Electroweak Uncertainty	Total
$H \to b\bar{b}, c\bar{c}$	$\sim 0.1\%$	$\sim 1-2\%$	$\sim 2\%$
svn up $H \to \tau^+\tau^-, \mu^+\mu^-$	-	$\sim 1-2\%$	$\sim 2\%$
$H \to gg$	$\sim 3\%$	$\sim 1\%$	$\sim 3\%$
$H \to \gamma\gamma$	$< 1\%$	$< 1\%$	$\sim 1\%$
$H \to Z\gamma$	$< 1\%$	$\sim 5\%$	$\sim 5\%$
$H \to WW^*/ZZ^* \to 4f$	$< 0.5\%$	$\sim 0.5\%$	$\sim 0.5\%$

Table 1-4. *Uncertainties on $M_H = 126$ GeV Standard Model branching ratios arising from the parametric uncertainties on α_s, m_b, and m_c and from theory uncertainties [7, 6]*

.

Decay	Theory Uncertainty (%)	Parametric Uncertainty (%)	Total Uncertainty on Branching Ratios (%)	Central Value
$H \to \gamma\gamma$	± 2.7	± 2.2	± 4.9	2.3×10^{-3}
$H \to b\bar{b}$	± 1.5	± 1.9	± 3.4	5.6×10^{-1}
$H \to \tau^+\tau^-$	± 3.5	± 2.1	± 5.6	6.2×10^{-2}
$H \to WW^*$	± 2.0	± 2.2	± 4.1	2.3×10^{-1}
$H \to ZZ^*$	± 2.0	± 2.2	± 4.2	2.9×10^{-2}
$H \to Z\gamma$	± 6.9	± 2.5	± 9.0	1.6×10^{-3}
$H \to \mu^+\mu^-$	± 4.0	± 2.5	± 5.9	2.1×10^{-4}

1.2.1 Higgs Coupling Fits

At the LHC, the rates of Higgs boson production and decay into particular final states are parametrized using strength parameters μ defined as the ratios between the observed rates and the expected ones in the standard model:

$$\mu = \frac{\sigma \times \mathrm{BR}}{(\sigma \times \mathrm{BR})_{\mathrm{SM}}}.$$

Table 1-5. *Uncertainties on $M_H = 126$ GeV Standard Model widths arising from the parametric uncertainties on α_s, m_b, and m_c and from theory uncertainties.*

Channel	$\Delta\alpha_s$	Δm_b	Δm_c	Theory Uncertainty	Total Uncertainty
$H \to \gamma\gamma$	0%	0%	0%	$\pm$1%	$\pm$1%
$H \to b\bar{b}$	$\pm$2.3%	$^{+3.3\%}_{-3.2\%}$	0%	$\pm$2%	$\pm$6%
$H \to \tau^+\tau^-$	0%	0%	0%	$\pm$2%	$\pm$2%
$H \to WW^*$	0%	0%	0%	$\pm$0.5%	$\pm$0.5%
$H \to ZZ^*$	0%	0%	0%	$\pm$0.5%	$\pm$0.5%

Table 1-6. *Projected future uncertainties in α_s, m_c, and m_b, compared with current uncertainties estimated from various sources.*

	Higgs X-section Working Group [5]	PDG [8]	non-lattice	Lattice (2013)	Lattice (2018)
$\Delta\alpha_s$	0.002	0.0007	0.0012 [8]	0.0006 [9]	0.0004
Δm_c (GeV)	0.03	0.025	0.013 [10]	0.006 [9]	0.004
Δm_b (GeV)	0.06	0.03	0.016 [10]	0.023 [9]	0.011

The deviations from the SM are implemented as scale factors ($\kappa' s$) of Higgs couplings relative to their SM values:

$$g_{Hff} = \kappa_f \cdot g^{\rm SM}_{Hff} = \kappa_f \cdot \frac{m_f}{v} \quad \text{and} \quad g_{HVV} = \kappa_V \cdot g^{\rm SM}_{HVV} = \kappa_V \cdot \frac{2m_V^2}{v}$$

such that $\kappa_f = 1$ and $\kappa_V = 1$ in SM. For example, at the LHC the $gg \to H \to \gamma\gamma$ rate can be written as

$$\sigma \times {\rm BR}(gg \to H \to \gamma\gamma) = \sigma_{\rm SM}(gg \to H) \cdot {\rm BR}_{\rm SM}(\ H \to \gamma\gamma) \cdot \frac{\kappa_g^2 \cdot \kappa_\gamma^2}{\kappa_H^2},$$

where κ_g and κ_γ are effective scale factors for the Hgg and $H\gamma\gamma$ couplings through loops. Additionally, κ_H^2 is the scale factor for the Higgs width:

$$\kappa_H^2 = \sum_X \kappa_X^2 {\rm BR}_{\rm SM}(H \to XX)\,,$$

where κ_X is the scale factor for the HXX coupling and ${\rm BR}_{\rm SM}(H \to XX)$ is the SM value of the $H \to XX$ decay branching ratio. The summation runs over all decay modes in the SM. This parameterization assumes that there is only one Higgs resonance, that the resonance is narrow, and that the Higgs interactions have the same tensor structure as the Standard Model interactions. Non-Standard Model Higgs decay modes will modify the total Higgs decay width and consequently rescale the branching ratios of all other known decay modes. In this case, κ_H^2 is modified to be

$$\kappa_H^2 = \sum_X \kappa_X^2 \frac{{\rm BR}_{\rm SM}(H \to XX)}{1 - {\rm BR}_{\rm BSM}}.$$

Here ${\rm BR}_{\rm BSM}$ is the total branching ratio of beyond-standard-model (BSM) decays.

1.2.2 Non-Standard Higgs Couplings due to New Physics

In this section, we survey a few models which can give Higgs couplings different from those of the Standard Model. All of these models contain new particles, so discovery of the new physics can result from direct detection of the new particles, or from the measurement of a deviation in the Higgs coupling from the Standard Model predictions [11]. We note that in order to be sensitive to a deviation, δ, the measurement must be made to a precision comparable to $\delta/2$ in order to obtain a 95% confidence level limit, or $\delta/5$ for a 5σ discovery of new physics. Coupling deviations in multiple production modes or final states can provide additional sensitivity to models that predict specific patterns.

1.2.2.1 One Parameter Model

One of the simplest extentions of the Standard Model is to add an $SU(2)$ singlet Higgs, S, which mixes with the usual Higgs doublet, Φ_{SM}, through a mixing term $\mid \Phi_{SM} \mid^2 \mid S \mid^2$. In some models that predict dark matter, the singlet, S, could arise from a hidden sector. There are two mass eigenstate Higgs particles: the observed 126 GeV Higgs boson, H, and a heavier Higgs particle, H_2. The Standard Model Higgs has couplings which are suppressed relative to the SM values [12],

$$\kappa_V \, = \, \kappa_F = \cos\alpha \tag{1.1}$$

where $V = W, Z$ and F denotes all the fermions. The value of $\sin\alpha$ is constrained by precision electroweak data and for $M_H \sim 1$ TeV, we must have $\sin^2\alpha < .12$ [11], which implies that in this model, the target for precision measurements of Higgs couplings is,

$$\kappa_V - 1 = \kappa_F - 1 < 6 \, \% \, . \tag{1.2}$$

1.2.2.2 Two Higgs Doublet Models

One of the most straightforward extensions of the Standard Model is the 2 Higgs doublet model. The 2HDMs contain 5 physical Higgs bosons: two neutral scalars, h and H, a pseudoscalar, A, and a charged Higgs boson, $H^{\pm}$. Models with a Z_2 symmetry can be constructed such that there are no tree level flavor changing neutral currents. The couplings of the Higgs bosons to fermions are described by two free parameters; the ratio of vacuum expectation values of the two Higgs doublets, $\tan\beta \equiv \frac{v_2}{v_1}$, and the mixing angle which diagonalizes the neutral scalar mass matrix, α. There are then four possible assignments of couplings for the light CP even Higgs boson, h^0, to fermions and gauge bosons relative to the Standard Model couplings, which are given in Table 1-7. The couplings to W and Z are always suppressed relative to the Standard Model couplings, while in model II and the flipped model, the couplings to $b's$ and τ's are enhanced at large $\tan\beta$.

Table 1-7. *Light Neutral Higgs, h, Couplings in the 2HDMs*

	I	II	Lepton Specific	Flipped
κ_V	$\sin(\beta-\alpha)$	$\sin(\beta-\alpha)$	$\sin(\beta-\alpha)$	$\sin(\beta-\alpha)$
κ_t	$\frac{\cos\alpha}{\sin\beta}$	$\frac{\cos\alpha}{\sin\beta}$	$\frac{\cos\alpha}{\sin\beta}$	$\frac{\cos\alpha}{\sin\beta}$
κ_b	$\frac{\cos\alpha}{\sin\beta}$	$-\frac{\sin\alpha}{\cos\beta}$	$\frac{\cos\alpha}{\sin\beta}$	$-\frac{\sin\alpha}{\cos\beta}$
κ_τ	$\frac{\cos\alpha}{\sin\beta}$	$-\frac{\sin\alpha}{\cos\beta}$	$-\frac{\sin\alpha}{\cos\beta}$	$\frac{\cos\alpha}{\sin\beta}$

Current limits on $\tan\beta$ and $\cos(\beta-\alpha)$ [13], along with projections for the high luminosity LHC and the $\sqrt{s} = 500$ GeV and $\sqrt{s} = 1000$ GeV ILC (assuming no deviations from the Standard Model) are given

in Ref. [14]. In model II and the flipped model, $\cos(\beta-\alpha)$ is already constrained to be near one, while larger deviations are possible in model I and the lepton specific model. Large values of $\tan\beta$ are as yet unconstrained by the data.

1.2.2.3 MSSM

The Higgs sector of the MSSM is a special case of the 2HDM and corresponds to model II. In the MSSM, the mixing angle, α, is related to the masses of the scalars. In the limit where the pseudoscalar A is much heavier than M_Z, the couplings take the simple form (called the decoupling limit) [15],

$$\begin{aligned}\kappa_V &\sim 1-\frac{2M_Z^4}{M_A^4}\cot^2\beta\\ \kappa_t &\sim 1-\frac{2M_Z^2}{M_A^2}\cot^2\beta\\ \kappa_b=\kappa_\tau &\sim 1+\frac{2M_Z^2}{M_A^2}\,.\end{aligned}\tag{1.3}$$

Studies of the MSSM suggest that with 300 fb^{-1} the LHC will be sensitive to $M_A\sim 400-500\ GeV$ for all values of $\tan\beta$ not excluded by LEP [16], giving as a target for the coupling precisions,

$$\begin{aligned}\kappa_V &\sim 1-.05\%\left(\frac{400}{M_A}\right)^4\cot^2\beta\\ \kappa_t &\sim 1-\mathcal{O}(10\%)\left(\frac{400\ GeV}{M_A}\right)^2\cot^2\beta\\ \kappa_b=\kappa_\tau &\sim 1+\mathcal{O}(10\%)\left(\frac{400\ GeV}{M_A}\right)^2.\end{aligned}\tag{1.4}$$

For large $\tan\beta$, the Higgs coupling to b's is enhanced and not only is the decay $h^0\to b\bar{b}$ enhanced, but the dominant production mechanism is the production in association with b's.

1.2.2.4 Composite Models

Composite models predict deviations in Higgs couplings due to higher dimension operators. Typically the deviations are $\mathcal{O}(v^2/f^2)$, where f is the scale associated with the new operators. Typically,

$$\begin{aligned}\kappa_V &\sim 1-3\%\left(\frac{1\ TeV}{f}\right)^2\\ \kappa_F &\sim 1-(3-9)\%\left(\frac{1\ TeV}{f}\right)^2\end{aligned}\tag{1.5}$$

1.2.2.5 New Couplings From Loops

Many models of new physics contain non -Standard Model particles which contribute via loops to the decays $H\to gg$, $H\to\gamma\gamma$ and/or $H\to Z\gamma$,[1] along with altering the $gg\to H$ production rate. These new particles give rise to the effective interactions parameterized by κ_g and κ_γ. Generically, one might expect these loop corrections to be $\mathcal{O}\left(\frac{v^2}{M^2}\right)\sim 6\%\left(\frac{1\ TeV}{M}\right)^2$, where M is the scale of the new physics effects. New heavy

[1] We will not discuss $H\to Z\gamma$ here, although this decay can receive significant corrections in new physics models.

fermions, such as top partners, and colored scalars can contribute to $H \to gg$ and $H \to \gamma\gamma$, while electrically charged scalars and heavy leptons can contribute to $H \to \gamma\gamma$. Below we examine some representative models, in order to get a feel for the size of the possible effects.

In Little Higgs models with T parity, the couplings scale with the top partner mass, M_T, and assuming the Higgs couplings to Standard Model particles are not changed, the loop induced couplings are [17],

$$\kappa_g = \kappa_\gamma \sim 1 - \frac{m_t^2}{M_T^2} \sim 1 - \mathcal{O}(8\%)\left(\frac{600\ GeV}{M_T}\right)^2. \tag{1.6}$$

In this scenario the production rate from gluon fusion is suppressed, as is the width into $\gamma\gamma$. Adding a vector-like $SU(2)$ doublet of heavy leptons does not change the $gg \to H$ production rate, but can give an enhancement in κ_γ of order $\sim 20\%$, but with large Yukawa couplings required [18].

Colored scalars, such as the stop particle in the MSSM, also contribute to both κ_g and κ_γ. If we consider two charge-$\frac{2}{3}$ scalars as in the MSSM, then for the stop much heavier than the Higgs boson,

$$\kappa_g = \kappa_\gamma \sim 1 + \frac{1}{4}\left(\frac{m_t^2}{m_{\tilde{t}_1}^2} + \frac{m_t^2}{m_{\tilde{t}_2}^2} - \frac{m_t^2 X_t^2}{m_{\tilde{t}_1} m_{\tilde{t}_2}}\right) \sim 1 + \mathcal{O}(17\%)\left(\frac{300\ GeV}{m_{\tilde{t}}}\right)^2 \text{ (for } X_t = 0), \tag{1.7}$$

where $X_t = \mid A_t - \mu \cot\beta \mid$ is the stop mixing parameter. If $X_t = 0$, the Higgs couplings to gluons and photons are always increased. If the stops are light, and the mixing is small, large enhancements are possible. In the MSSM, there are other loop contributions to the $H\gamma\gamma$ and Hgg couplings which have been extensively studied. Enhancements in the $H \to \gamma\gamma$ coupling can be obtained with light staus and large mixing, with effects on the order of $\sim 25\%$ [19].

In Table 1-8, we summarize the generic size of coupling modifications when the scale of new physics is consistently taken to be $M \sim 1$ TeV.

Table 1-8. *Generic size of Higgs coupling modifications from the Standard Model values when all new particles are $M \sim 1$ TeV and mixing angles satisfy precision electroweak fits.*

	κ_V	κ_b	κ_γ
Singlet Mixing	$\sim 6\%$	$\sim 6\%$	$\sim 6\%$
2HDM	$\sim 1\%$	$\sim 10\%$	$\sim 1\%$
Decoupling MSSM	$\sim -0.0013\%$	$\sim 1.6\%$	$< 1.5\%$
Composite	$\sim -3\%$	$\sim -(3-9)\%$	$\sim -9\%$
Top Partner	$\sim -2\%$	$\sim -2\%$	$\sim -3\%$

1.2.3 Theory Uncertainties on LHC Higgs Production

The uncertainty on Higgs production has been studied by the LHC Higgs cross section working group for the various channels and is summarized in Table 1-9 [20]. These uncertainties must be included in extractions of the scale factors κ_i from LHC data. The error includes factorization/renormalization scale uncertainty and the correlated uncertainty from α_s and the PDF choice, which are added linearly. The scale uncertainty on the gluon fusion rate is $\sim \pm 10\%$, which can potentially be significantly reduced with the inclusion of recent approximate NNNLO results [21]. In addition, there are further uncertainties from binning the Higgs data into $0, 1$ and 2 jet bins. The theory error on the 1 jet bin will be significantly reduced with the inclusion of the NNLO result for Higgs plus one jet [22] and by resumming jet veto effects.

Table 1-9. *Theory Uncertainties for $m_H = 125$ GeV Higgs Production at the LHC [20].*

Process	Cross Section (pb)
Gluon fusion	$49.85^{+19.6\%}_{-14.6\%}$
VBF	$4.18^{+2.8\%}_{-3\%}$
WH	$1.504^{+4.1\%}_{-4.4\%}$
ZH	$.883^{+6.4\%}_{-5.5\%}$

1.2.4 Theory Uncertainties on e^+e^- Higgs Production

1.2.5 Measurements at Hadron Colliders and Projections at LHC

In pp or $p\bar{p}$ collisions, the Higgs boson can be produced through the following four main processes: gluon-gluon fusion $gg \to H$ through a heavy quark triangular loop (ggF), vector boson fusion (VBF), associated production with a vector boson W or Z (VH), and production in association with a pair of top quarks ($t\bar{t}H$). The cross sections of these processes in pp collisions at $\sqrt{s} = 7, 8$ and 14 TeV are listed in Table 1-10.

Table 1-10. *Higgs boson production cross sections of different processes at 7, 8 and 14 TeV of pp collisions. These cross sections are taken from Ref. [23].*

$\sqrt{s}$	Cross sections in pb $m_H = 125$ GeV				
(TeV)	ggF	VBF	WH	ZH	$t\bar{t}H$
7	15.1	1.22	0.579	0.335	0.086
8	19.5	1.58	0.697	0.394	0.130
14	49.9	4.18	1.50	0.883	0.611

Since the discovery of the ∼126 GeV Higgs-like particle in Summer 2012, the LHC experiments have focused on the measurements of its production rates and couplings. Both ATLAS and CMS have released results based on the LHC Run 1 dataset of ∼5 fb^{-1} at 7 TeV and ∼20 fb^{-1} at 8 TeV. These results strongly suggest that the new particle is a Higgs boson and its properties are consistent with the expectations of the SM Higgs boson. After a two-year shutdown, the LHC is scheduled to operate again in 2015 at $\sqrt{s} = 14$ TeV. It is expected to deliver 300 fb^{-1} to each experiment by 2022. With the planned high luminosity upgrade, an integrated luminosity of 3000 fb^{-1} is foreseen by 2030. The increased luminosity will significantly increase the measurement precision of the Higgs boson properties. The current results are briefly summarized and the projected precisions are presented below.

1.2.6 Production Rates and Coupling Fits

Table 1-11 summarizes the current measurements of overall rates from the Tevatron [24], ATLAS [25], and CMS [26], separately for the five main decay modes. These measurements are generally in good agreements with the SM prediction of $\mu = 1$. In addition to the measurements by decay modes, measurements by production processes have also been done for some processes through categorizing Higgs candidate events. From example, VH candidates can be selected by the presence of additional leptons from V decays while VBF candidates are tagged by two forward jets. Searches for rare decays of $H \to \mu\mu$ [27] and $H \to Z\gamma$ [28,29]

as well as $H \rightarrow$invisible in ZH [30] (+CMS-PAS-HIG-13-018) have also been performed. Upper limits of these searches are also shown in Table 1-11.

Table 1-11. *Summary of the measured production rates or 95% CL upper limits relative to their SM predictions from hadron colliders by decay channels. The last line shows the upper limit on the branching ratio of Higgs to invisible decays from the search of ZH with $H \rightarrow$invisible. The ATLAS combined rate includes only $H \rightarrow \gamma\gamma$, ZZ^* and WW^* decays.*

Decay mode	Tevatron ($m_H = 125$ GeV)	ATLAS ($m_H = 125.5$ GeV)	CMS ($m_H = 125.7$ GeV)
$H \rightarrow \gamma\gamma$	$5.97^{+3.39}_{-3.12}$	$1.55 \pm 0.23(\text{stat}) \pm 0.15(\text{syst})$	0.77 ± 0.27
$H \rightarrow ZZ^*$	–	$1.43 \pm 0.33(\text{stat}) \pm 0.17(\text{syst})$	0.92 ± 0.28
$H \rightarrow WW^*$	$0.94^{+0.85}_{-0.83}$	$0.99 \pm 0.21(\text{stat}) \pm 0.21(\text{syst})$	0.68 ± 0.20
$H \rightarrow \tau\tau$	$1.68^{+2.28}_{-1.68}$	–	1.10 ± 0.41
$H \rightarrow b\bar{b}$	$1.59^{+0.69}_{-0.72}$	$0.2 \pm 0.5(\text{stat}) \pm 0.4(\text{syst})$	1.15 ± 0.62
Combined	$1.44^{+0.59}_{-0.56}$	$1.33 \pm 0.14(\text{stat}) \pm 0.15(\text{syst})$	0.80 ± 0.14
	95% CL observed (expected) upper limit		
$H \rightarrow \mu\mu$	–	< 9.8 $(8.2)^\dagger$	
$H \rightarrow Z\gamma$	–	< 13.5 $(18.2)^\dagger$	$4 - 25(5 - 16)\%^\ddagger$
BR_{inv}	–	< 65 $(84)\%^\dagger$	< 75 $(91)\%^\dagger$

$\dagger$ at $m_H = 125$ GeV; $\ddagger$ for $m_H = 120 - 160$ GeV.

Higgs couplings to fermions and vector bosons are determined following the procedure discussed in section 1.2.1. Given the current statistics, fits to Higgs couplings to individual leptons, quarks and vector bosons are not meaningful and therefore have not been done so far. However fits have been performed with reduced number of parameters under various assumptions. Results of these fits can be found in Ref. [25, 26] and Fig. 1-1 illustrates some representative results.

1.2.7 LHC Projections

Precision measurements of the properties of the Higgs boson will be a central topic for the LHC physics program in the foreseeable future. The high-luminosity LHC is not only an energy frontier machine, it is also an intensity frontier collider. The expected large statistics will significantly improve the precision of the current measurements of couplings to fermions and vector bosons.

The LHC is expected to deliver 300 fb^{-1} at 14 TeV before the high-luminosity upgrade and 3000 fb^{-1} afterward, representing factors of 15 and 150 increases in statistics from luminosity alone from the current 7 and 8 TeV datasets. The higher pp collision energy will also increase the Higgs production cross sections by a factor of 2.6 or larger. The numbers of predicted Higgs events are shown in Table 1-12 for different production processes and decay modes. LHC experiments generally have good sensitivities to final states with electrons, muons or photons. $H \rightarrow \tau\tau$ events are identified through $\tau \rightarrow e$ or μ decays and also $\tau \rightarrow$hadrons decays in the case of VBF production. For $H \rightarrow b\bar{b}$ decays, most of their sensitivities are derived from the VH ($V = W, Z$) production with the leptonic decays of V. The signal-background ratios are strongly dependent on analyses. For $H \rightarrow \gamma\gamma$, the S/B ranges from $\sim 3\%$ for the inclusive analysis to

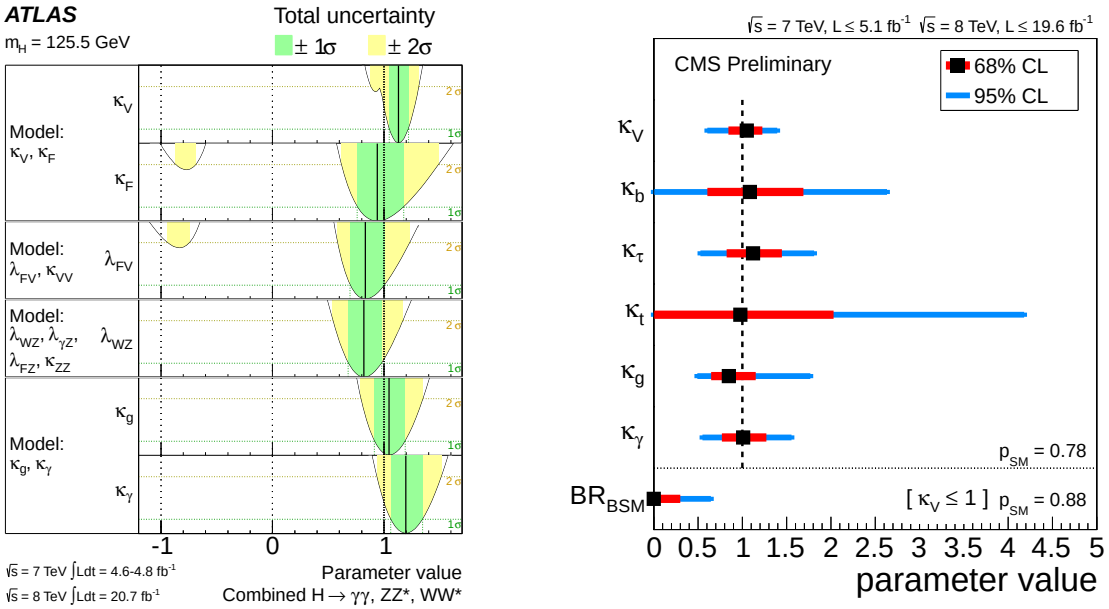

Figure 1-1. *Left: summary of the ATLAS coupling scale factor measurements for different models. The solid vertical lines are the best-fit values while the dark- and light-shaded band represent the total $\pm 1\sigma$ and $\pm 2\sigma$ uncertainties. The curves are distributions of the likelihood ratios. Right: summary of the CMS fits for deviations in the coupling for the generic six-parameter model including effective loop couplings. The result of the fit when extending the model to allow for beyond-SM decays while restricting the coupling to vector bosons to not exceed unity ($\kappa_V \leq 1.0$) is also shown.*

$\sim 20\%$ for some exclusive analyses with selection efficiencies $\epsilon \sim 40\%$. The $H \to ZZ^* \to 4\ell$ analysis has a much smaller background and therefore a S/B ratio of better than 2:1 with $\epsilon \sim 30\%$. On the other hand, the $H \to WW^* \to \ell\nu\ell\nu$ analysis has a $S/B \sim 10\%$ with $\epsilon \sim 5\%$. For rare decays such as $H \to \mu\mu$ and $H \to Z\gamma \to \ell\ell\gamma$, the S/B is $\sim 0.5\%$ with $\epsilon \sim 40\%$.

Both ATLAS and CMS experiments have projected their sensitivities to high luminosities [31,32] with varying assumptions of detector and analysis performance. Arguably the most significant challenge is to deal with the high pileup that will come along with the high luminosity. The average number of interactions per beam crossing is expected to reach 140 compared with current 20. However, the upgraded detectors are expected to mitigate most of the adverse impact from the higher pileup and maintain (in some cases exceed) the performance of the current detectors.

ATLAS has taken the approach to estimate sensitivities using fast parametric simulations. Effectively all analyses will have to be repeated and consequently it takes longer to converge. At the time of this report writing, not all major analyses have converged. On the other hand, CMS has taken a different approach, making projections based on the analyses of 7 and 8 TeV data with varying assumptions. Unless noted, CMS projections are taken as the expected LHC per-experiment precisions. Table 1-13 summarizes the expected precisions on the signal strengths of different Higgs decay modes as well as 95% CL upper limit on the branching ratio of Higgs to invisible decay [32]. These projections are based on the analysis of 7 and 8

Table 1-12. *The numbers of predicted Higgs events produced in 3000 fb^{-1} at 14 TeV in different production processes and decay modes for $m_H = 125$ GeV. Experimental sensitivity to these productions and decays varies widely, see text. Here $\ell = e, \mu$.*

	ggF	VBF	VH	$t\bar{t}H$	Total
Cross section (pb)	49.9	4.18	2.38	0.611	57.1
			Numbers of events in 3000 fb^{-1}		
$H \to \gamma\gamma$	344,310	28,842	16,422	4,216	393,790
$H \to ZZ^* \to 4\ell$	17,847	1,495	851	219	20,412
$H \to WW^* \to \ell\nu\ell\nu$	1,501,647	125,789	71,622	18,387	1,717,445
$H \to \tau\tau$	9,461,040	792,528	451,248	115,846	10,820,662
$H \to b\bar{b}$	86,376,900	7,235,580	4,119,780	1,057,641	98,789,901
$H \to \mu\mu$	32,934	2,759	1,570	403	37,667
$H \to Z\gamma \to \ell\ell\gamma$	15,090	1,264	720	185	17,258
$H \to$ all	149,700,000	12,540,000	7,140,000	1,833,000	171,213,000

Table 1-13. *Expected relative precisions per experiment on the signal strengths of different Higgs decay final states as well as the 95% CL upper limit on the Higgs branching ratio to the invisible decay from the ZH search. The $H \to \mu\mu$ estimates are from ATLAS [31] while the rest are from CMS [32]. The ranges represent two scenarios of systematic uncertainties, see text.*

$\int \mathcal{L}dt$	Higgs decay final state							
(fb^{-1})	$\gamma\gamma$	WW^*	ZZ^*	$b\bar{b}$	$\tau\tau$	$\mu\mu$	$Z\gamma$	$\mathrm{BR}_{\mathrm{inv}}$
300	$6-12\%$	$6-11\%$	$7-11\%$	$11-14\%$	$8-14\%$	$51-53\%$	$62-62\%$	$<17-28\%$
3000	$4-8\%$	$4-7\%$	$4-7\%$	$5-7\%$	$5-8\%$	$17-21\%$	$20-24\%$	$<6-17\%$

TeV data, not all final states have been explored. They are expected to improve once more final states are included. Two scenarios of systematics are considered:

- *conservative scenario* assumes no reduction in systematics as the integrated luminosity is increased;
- *optimistic scenario* assumes the theoretical systematics are reduced by a factor of two while experimental systematics scale with the inverse of the square-root of the luminosity, *i.e.*, $1/\sqrt{\mathcal{L}}$.

The ranges of the projections in the table represent these two scenarios.

Table 1-14 summarizes the expected precision on the Higgs couplings for the two aforementioned assumptions of systematic uncertainties from the fit to a generic 7-parameter model. These 7 parameters are κ_γ, κ_g, κ_W, κ_Z, κ_u, κ_d and κ_ℓ. In this parameter set, κ_γ and κ_g parametrize potential new physics in the loops of the $H\gamma\gamma$ and Hgg couplings. $\kappa_u \equiv \kappa_t = \kappa_c$, $\kappa_d \equiv \kappa_b = \kappa_s$ and $\kappa_\ell \equiv \kappa_\tau = \kappa_\mu$ parametrize deviations to up-and down-type quarks and charged leptons respectively assuming fermion family universality. Only SM

productions and decays are considered in the fit. The derived precisions on the Higgs total width are also included. The expected precision ranges from $5-15\%$ for 300 fb^{-1} and $2-10\%$ for 3000 fb^{-1}. They are limited by systematic uncertainties, particularly theoretical uncertainties on production and decay rates. Statistical uncertainties are below one percent in most cases. Note that the sensitivity to κ_u is derived from the $t\bar{t}H$ production process and only $H \to \gamma\gamma$ and $H \to b\bar{b}$ decays have been included in the projection.

The fit is extended to allow for BSM decays while restricting the Higgs coupling to vector bosons not to exceed their SM values ($\kappa_W, \kappa_Z \leq 1$). The resulting upper limit on the branching ratio of BSM decay is included in the table. Note that the $\mathrm{BR}_{\mathrm{BSM}}$ limit is derived from the visible decays of Table 1-13 and is independent of the limit on $\mathrm{BR}_{\mathrm{inv}}$ from the search of ZH with $H \to$invisible.

Also listed in the Table 1-14 are the expected precisions on $\kappa_{Z\gamma}$ and κ_μ, coupling scale factors for $H \to Z\gamma$ and $H \to \mu\mu$ decay vertices. The projection for κ_μ is estimated from the $H \to \mu\mu$ rate precision reported in Table 1-13 as neither ATLAS nor CMS reported its projection. Given the small branching ratios of the two decays in the SM, they have negligible impact on the 7-parameter fit.

Table 1-14. *Expected per-experiment precision of Higgs boson couplings to fermions and vector bosons with 300 fb^{-1} and 3000 fb^{-1} integrated luminosity at the LHC. The 7-parameter fit assumes the SM productions and decays as well as the generation universality of the couplings ($\kappa_u \equiv \kappa_t = \kappa_c$, $\kappa_d \equiv \kappa_b = \kappa_s$ and $\kappa_\ell \equiv \kappa_\tau = \kappa_\mu$). The precision on the total width Γ_H is derived from the precisions on the couplings. The range represents spread from conservative and optimistic scenarios, see text.*

Coupling parameter	300 fb^{-1}	3000 fb^{-1}
7-parameter fit		
κ_γ	$5-7\%$	$2-5\%$
κ_g	$6-8\%$	$3-5\%$
κ_W	$4-6\%$	$2-5\%$
κ_Z	$4-6\%$	$2-4\%$
κ_u	$14-15\%$	$7-10\%$
κ_d	$10-13\%$	$4-7\%$
κ_ℓ	$6-8\%$	$2-5\%$
Γ_H	$12-15\%$	$5-8\%$
additional measurements		
$\kappa_{Z\gamma}$	$41-41\%$	$10-12\%$
κ_μ	$34-35\%$	$9-11\%$
$\mathrm{BR}_{\mathrm{BSM}}$	$< 14-18\%$	$< 7-11\%$

Apart from contributions from ATLAS and CMS collaborations, several independent studies have been performed. Ref. [33] investigates top-quark Yukawa coupling through the $t\bar{t}H$ production and $H \to WW^*$ decay. The authors estimate that the κ_t can be measured with a precision of $14-16\%$ and $6-9\%$ in 300 and 3000 fb^{-1} from this final state alone, comparable to, but independent of, the κ_u ($\equiv \kappa_t$) precision shown in Table 1-14. Combining the two, a precision of $\sim 5\%$ on κ_t is obtainable.

The rare decays $H \to V\gamma$, where V denotes a vector meson such as the J/ψ or the $\Upsilon(1S)$ which subsequently decays via $V \to \ell^+\ell^-$, provide a handle on otherwise difficult-to measure properties of the Higgs boson [34].

Quantum interference between the two production mechanisms that contribute to this decay enhances its sensitivity to the $H\bar{Q}Q$ coupling, and potentially allows the $H\bar{c}c$ coupling to be constrained directly by measurement of the branching ratio for $H \to J/\psi\,\gamma$.

1.2.8 Projections for e^+e^- machines

The measurements of Higgs couplings in e^+e^- collisions benefit from a clean experimental environment, precisely known E_{cm} and initial state polarization, and well predicted backgrounds many orders of magnitude below the challenging QCD backgrounds of the hadron colliders. The e^+e^- collider is a well-studied Higgs factory. Although most studies in the past decades focus on linear colliders [35, 36, 37, 38, 39, 40, 41, 42, 43], the experimentally accessible Higgs physics at a given center-of-mass energy depends only weakly whether it is a linear or circular machine [44, 45], with differences driven primarily by luminosity and possible number of detector interaction points. In the measurement of Higgs couplings at a linear collider, the very small beam size at the interaction point and time structure of the beams allowing vertex detectors to be operated in a pulsed mode would benefit flavor tagging in $H \to b\bar{b}$ and $c\bar{c}$ decays. Beamstrahlung effects, resulting in collisions at less than $2E_{\rm beam}$, tend to be less in a circular e^+e^- machine than at a linear collider, although the impact on Higgs precision measurements is small.

The measurement of couplings naturally divides according to the production of process. At relatively low $\sqrt{s}$ energies of $\simeq$ 250 – 350 GeV, the Higgs-strahlung process $e^+e^- \to ZH$ dominates and tagging the Z allows for a model-independent separation of the recoil Higgs decays. For $\sqrt{s} \geq 500$ GeV, the W-fusion mode $e^+e^- \to \nu_e\bar{\nu}_e H$ dominates and grows with $\sqrt{s}$ allowing for better precision of the WW coupling and higher statistics for other decay modes, including rare decays. These higher energies also provide access to the top quark Yukawa coupling through $e^+e^- \to t\bar{t}H$ and the Higgs trilinear self-coupling via double-Higgs production: $e^+e^- \to ZHH$ and $\nu_e\bar{\nu}_e HH$ (discussed in section 1.3.3).

1.2.8.1 Collision energies 250 – 350 GeV

A key decay mode is $e^+e^- \to ZH$ where events can be detected inclusively, completely independent of the Higgs decay mode by tagging the Z via $Z \to \mu^+\mu^-$ and e^+e^- and requiring that the recoil mass is consistent with the Higgs boson mass. The normalization of this rate then allows a precision measurement of $\sigma(ZH)$ that is in turn proportional to g^2_{ZZ}. With this in hand, the other Z decay modes can be employed and measurements of $\sigma(ZH) \cdot \mathrm{BR}$ lead to *absolute* measurements of *all* possible branching fractions, including invisible Higgs decays and decay modes undetectable at the LHC due to large backgrounds. Note that the uncertainty on $\sigma(ZH)$ at $\sqrt{s} = 250$ GeV eventually limits the precisions on the branching fraction measurements. Assuming a single resonance,

$$\Gamma_H = \Gamma(H \to ZZ)/\mathrm{BR}(H \to ZZ) \propto \sigma(ZH)/\mathrm{BR}(H \to ZZ) \tag{1.8}$$

allowing a model independent extraction of the width of the Higgs, free from confusion of whether there is new physics in couplings or in new decay modes. At increasing $\sqrt{s}$, starting at, e.g., the 350 GeV TLEP or the initial 350 GeV phase of CLIC, there is enough rate in the WW-fusion process so that using:

$$\Gamma_H = \Gamma(H \to WW^*)/\mathrm{BR}(H \to WW^*), \tag{1.9}$$

$\Gamma(H \to WW^*)$ can be determined by measuring the cross section for $e^+e^- \to \nu_e\bar{\nu}_e H$, giving another handle on the total Higgs width. This is even more true of the higher energies at 500 GeV and beyond. Such a rich program of Higgs physics can be carried out at any of the e^+e^- machines with sufficient luminosity.

Full simulations of such events in the ILD [46] and SiD [47] detectors [48] have been performed over many years, including all physics backgrounds. Overlays of $\gamma\gamma \to$ hadrons and beam-induced backgrounds have

also been included for studies at ILC [49, 50] and most CLIC [51] studies. A full simulation of the CMS detector has been used to make projections of precisions attainable at TLEP [52,53,45], with extrapolations made for $H \to c\bar{c}$ and gg. Results are collated in Table 1-15.

1.2.8.2 Collision energies ≥ 500 GeV

The e^+e^- collisions at $\sqrt{s} \geq 500$ GeV are the exclusive realm of linear colliders (more speculative rings such as the Very Large Lepton Collider (VLLC) with circumferences greater than 100 km are not considered here). At these higher energies, large samples of events from both the WW and ZZ fusion processes lead to improved precision on all the branching fractions, and allow probing of rare decays such as $H \to \mu^+\mu^-$. Equally important, the relation of Eq. 1.9 provides a significantly improved measurement of the total Higgs width consequently improving the precision on *all* the branching fractions and model-independent extraction of the associated Higgs couplings.

Higher energies also open up the production channel $e^+e^- \to t\bar{t}H$. Significant enhancements of this cross section near threshold due to $t\bar{t}$ bound states [54] implies that the measurement of the top Yukawa coupling g_t may already be possible at $\sqrt{s} = 500$ GeV [55], but has more sensitivity at the higher energy operating points of the ILC and CLIC where the signal cross section is larger and $t\bar{t}$ background is smaller.

Studies using full simulations of detectors at the ILC and CLIC [49, 50, 51] result in coupling precisions presented in Table 1-15.

1.2.8.3 Model Independent Coupling Fits

To provide a true representation of the lepton-collider potential, as well as a comparison between e^+e^- options on an equal fitting, Table 1-15 shows the precision on couplings from global fits without any assumptions on or between g_W and g_Z, nor with any assumptions on the saturation of the total width by invisible decays. The inputs to these model-independent fits are taken from Table 1-18.

1.2.9 Projections for a photon collider operating on the Higgs resonance

A stand-alone photon collider operating on the Higgs resonance could be constructed using laser Compton backscattering off of e^-e^- beams at $\sqrt{s_{ee}} = 160$ GeV [56, 57, 58]. The photon collider could measure $\Gamma_{\gamma\gamma} \times \mathrm{BR}(H \to X)$ from event rates in various final states. Table 1-16 summarizes the anticipated sensitivities to production times decay rates, corresponding to 50,000 raw $\gamma\gamma \to H$ events [58].

Model-independent Higgs coupling extraction is not possible unless input from another collider can be provided. A model-independent measurement of $\mathrm{BR}(H \to bb)$ from an e^+e^- collider yields a 2% measurement of $\Gamma_{\gamma\gamma}$ can be obtained [58], corresponding to 1% precision on κ_γ. Combining this with the rate measurement for $\gamma\gamma \to H \to \gamma\gamma$ yields a measurement of the total Higgs width to 13% [58].

1.2.10 Projections for a muon collider operating on the Higgs resonance

A muon collider can produce the Higgs boson as an s-channel resonace, $\mu^+\mu^- \to H \to X$. By scanning the beam energy across the resonance, the Higgs total width can be measured directly (see Sec. 1.5.3). Combinations of production and decay couplings can then be extracted from measurements of the event rates in various final states.

Sensitivities have been studied for an idealized detector design including full simulation in Ref. [59]. Important components of the detector are tungsten shielding cones at high rapidity and precise timing to reduce beam-related backgrounds.

The studies in [59] simulated Higgs events and Drell-Yan backgrounds for a beam energy scan across the Higgs peak. Precisions on the $\mu\mu \to H \to X$ Higgs signal rates in each channel and the mass and width resolution depend on the beam energy spread, total luminosity, and scan strategy. Table 1-17 summarizes the precisions achievable from a 5-point energy scan centered on the Higgs resonance at $\sqrt{s} \sim 126$ GeV, with a scan point separation of 4.07 MeV. The run scenario assumes 1 Snowmass year (10^7 s) at 1.7×10^{31} cm^{-2}s^{-1} plus 5 Snowmass years at 8.0×10^{31} cm^{-2}s^{-1} and a beam energy resolution of $R = 4 \times 10^{-5}$ (the beam energy spread should be measurable to high precision using muon precession in the accelerator field). Perfect b-tagging efficiency and purity were assumed. An alternate strategy of sitting on the Higgs peak increases the Higgs yield and would slightly improve the rate measurements.

These rates are proportional to $\mathrm{BR}(H \to \mu\mu) \times \mathrm{BR}(H \to X) \propto \kappa_\mu^2 \kappa_X^2 / \Gamma_H^2$. Products of couplings $\kappa_\mu \kappa_X$ can be extracted using the direct measurement of the Higgs width Γ_H from the lineshape scan, with an estimated uncertainty $\Delta\Gamma_H = 4.3\%$ (see also Sec. 1.5.3). Model-independent Higgs coupling measurements are not possible unless $\sigma(\mu\mu \to H \to \mu\mu) \propto \kappa_\mu^4 / \Gamma_H^2$ can be measured. Making the assumption of generation universality, $\kappa_\ell \equiv \kappa_\mu = \kappa_\tau$, would allow κ_b, κ_W, and κ_ℓ to be extracted, but the uncertainty is dominated by the large ($\sim$60%) uncertainty on the $\mu\mu \to H \to \tau\tau$ rate.

1.2.11 Comparison of Precision at Different Facilities

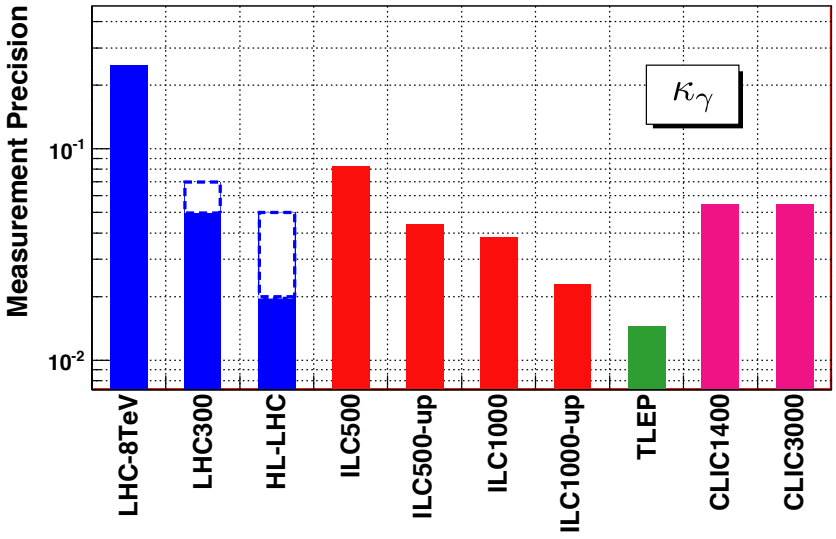

Figure 1-2. *Measurement precision on κ_γ at different facilities.*

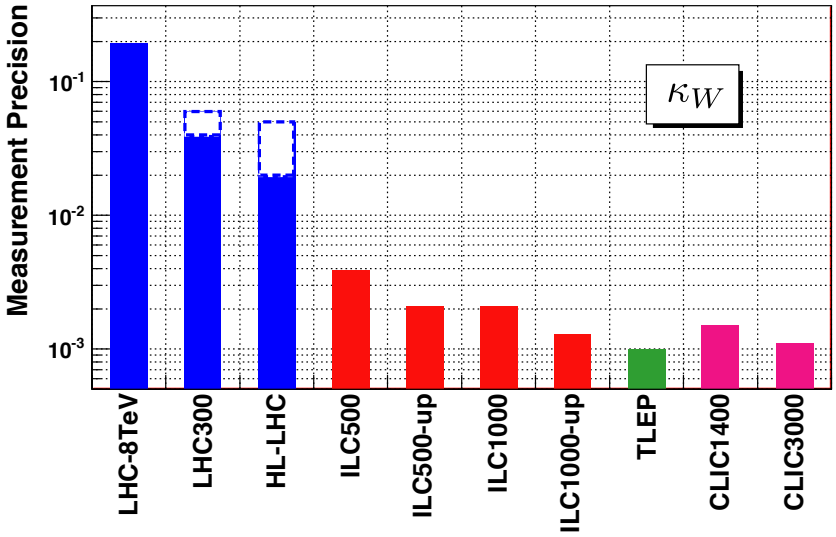

Figure 1-3. *Measurement precision on κ_W at different facilities.*

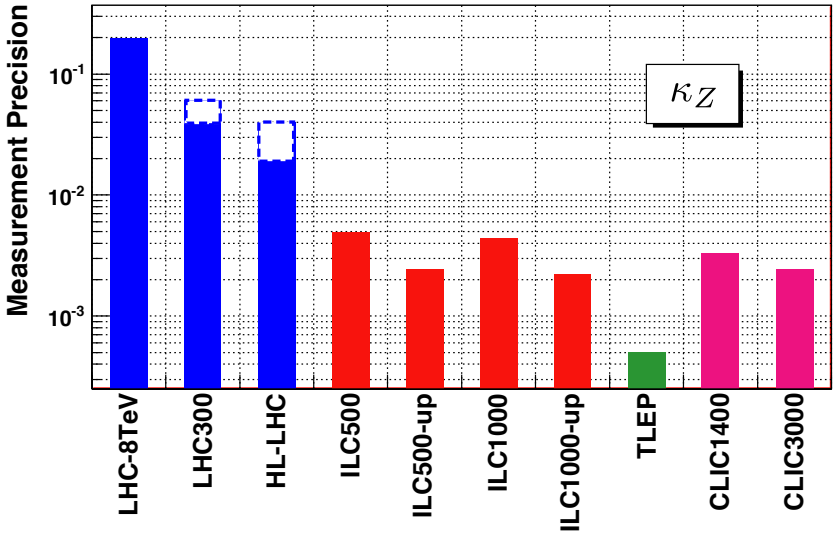

Figure 1-4. *Measurement precision on κ_Z at different facilities.*

Table 1-15. *Uncertainties on couplings as determined in a completely model-independent fit for different e^+e^- facilities. Precisions reported in a given column include in the fit all measurements at lower energies at the same facility. ‡ILC luminosity upgrade assumes an extended running period on top of the low luminosity program and cannot be directly compared to TLEP and CLIC numbers without accounting for the additional running period.*

Facility		ILC		ILC(LumiUp)	TLEP (4 IP)			CLIC	
$\sqrt{s}$ (GeV)	250	500	1000	250/500/1000	240	350	350	1400	3000
$\int \mathcal{L}dt$ (fb^{-1})	250	+500	+1000	1150+1600+2500‡	10000	+2600	500	+1500	+2000
$P(e^-, e^+)$	$(-0.8, +0.3)$	$(-0.8, +0.3)$	$(-0.8, +0.2)$	(same)	$(0, 0)$	$(0, 0)$	$(-0.8, 0)$	$(-0.8, 0)$	$(-0.8, 0)$
Γ_H	11%	5.9%	5.6%	2.7%	1.9%	1.0%	9.2%	8.5%	8.4%
BR_{inv}	$< 0.69\%$	$< 0.69\%$	$< 0.69\%$	$< 0.32\%$	0.19%	$< 0.19\%$	tbd	tbd	tbd
κ_γ	18%	8.4%	4.1%	2.4%	1.7%	1.5%	–	5.9%	<5.9%
κ_g	6.4%	2.4%	1.8%	0.93%	1.1%	0.8%	4.1%	2.3%	2.2%
κ_W	4.8%	1.4%	1.4%	0.65%	0.85%	0.19%	2.6%	2.1%	2.1%
κ_Z	1.3%	1.3%	1.3%	0.61%	0.16%	0.15%	2.1%	2.1%	2.1%
κ_μ	–	–	16%	10%	6.4%	6.2%	–	11%	5.6%
κ_τ	5.7%	2.4%	1.9%	0.99%	0.94%	0.54%	4.0%	2.5%	<2.5%
κ_c	6.8%	2.9%	2.0%	1.1%	1.0%	0.71%	3.8%	2.4%	2.2%
κ_b	5.3%	1.8%	1.5%	0.74%	0.88%	0.42%	2.8%	2.2%	2.1%
κ_t	–	14%	3.2%	2.0%	–	13%	–	4.5%	<4.5%

Table 1-16. *Photon collider precisions on Higgs production rates into various final states X, using a sample of 50,000 $\gamma\gamma \to H$ events, from Ref. [58]. The WW^* analysis includes only leptonic final states and the ZZ^* analysis includes only $\ell\ell qq$ final states.*

Final state	$b\bar{b}$	WW^*	$\tau\tau$	$c\bar{c}$	gg	$\gamma\gamma$	ZZ^*	$Z\gamma$	$\mu\mu$
$\Gamma_{\gamma\gamma} \times \mathrm{BR}(H \to X)$	1%	3%	?	–	–	12%	6%	20%	38%

Table 1-17. *Muon collider statistical precisions on Higgs production rates into various final states X from a 5-point energy scan centered at m_H with a combined yield of 39,000 Higgs bosons. The $\tau\tau$ uncertainty is an average of asymmetric uncertainties. The rates are proportional to $\mathrm{BR}(H \to \mu\mu) \times \mathrm{BR}(H \to X) \propto \kappa_\mu^2 \kappa_X^2 / \Gamma_H^2$.*

Final state	$b\bar{b}$	WW^*	$\tau\tau$	$c\bar{c}$	gg	$\gamma\gamma$	ZZ^*	$Z\gamma$	$\mu\mu$	Γ_H	m_H
$\sigma(\mu\mu \to H \to X)$	9%	5%	60%	–	–	–	–	–	–	4.3%	0.06 MeV

Table 1-18. *Precisions of measured $\sigma \cdot \mathrm{BR}$ inputs for e^+e^- Higgs factories for complete programs: ILC: 250 fb^{-1} at 250 GeV, 500 fb^{-1} at 500 GeV, 1000 fb^{-1} at 1000 GeV; ILC LumiUp: adding 1150 fb^{-1} at 250 GeV, 1600 fb^{-1} at 500 GeV, 2500 fb^{-1} at 1000 GeV; CLIC: 500 fb^{-1} at 350 GeV, 1500 fb^{-1} at 1.4 TeV, 3000^{-1} at 3.0 TeV; TLEP (4 IPs): 10000 fb^{-1} at 240 GeV, 2600 fb^{-1} at 350 GeV. The CLIC numbers are assuming increased WW cross sections above 1 TeV with $(-0.8, 0)$ polarization of (e^-, e^+) (a factor of approximately 1.8 above the unpolarized case). †CLIC at 350 GeV. ‡ILC luminosity upgrade assumes an extended running period on top of the low luminosity program and cannot be directly compared to TLEP and CLIC numbers without accounting for the additional running period.*

	ILC 250/500/1000 GeV		ILC LumiUp‡ 250/500/1000 GeV		CLIC 1.4/3.0 TeV		TLEP (4 IPs)	
	ZH	$\nu\nu H$	ZH	$\nu\nu H$	$ZH^\dagger$	$\nu\nu H$	ZH	$\nu\nu H$
Inclusive	2.5/–/–%	–	1.2/–/–%	–	4.2%†	–	0.4%	–
$H \to \gamma\gamma$	29-38%	–/20-26/7-10%	16/19/–%	–/13/5.4%	–	11%/tbd	3.0%	tbd
$H \to gg$	7/11/–%	–/4.1/2.3%	3.3/6.0/–%	–/2.3/1.4%	6%	1.4/1.4%	1.4%	tbd
$H \to ZZ^*$	19/25/–%	–/8.2/4.1%	8.8/14/–%	–/4.6/2.6%	tbd	2.3/1.5%	3.1%	tbd
$H \to WW^*$	6.4/9.2/–%	–/2.6/1.6%	3.0/5.1/–%	–/1.4/1.0%	2%	0.75/0.5%	0.9%	tbd
$H \to \tau\tau$	4.2/5.4/–%	–/14/3.5%	2.0/3.0/–%	–/7.8/2.2%	5.7%	2.8%/tbd	0.7%	tbd
$H \to b\bar{b}$	1.2/1.8/–%	11/0.66/0.32%	0.56/1.0/–%	4.9/0.37/0.20%	1%	0.23/0.15%	0.2%	0.6%
$H \to c\bar{c}$	8.3/13/–%	–/6.2/3.1%	3.9/7.2/–%	–/3.2/2.0%	5%	2.2/2.0%	1.2%	tbd
$H \to \mu\mu$	–	–/–/31%	–	–/–/20%	–	21/12%	13%	tbd
	$t\bar{t}h$		$t\bar{t}h$		$t\bar{t}h$		$t\bar{t}h$	
$h \to b\bar{b}$	–/35/7.8%		–/20/4.9%		8%/tbd		–	

Table 1-19. *Expected precisions on the Higgs couplings and total width from a constrained 7-parameter fit assuming no non-SM production or decay modes. The fit assumes generation universality ($\kappa_u \equiv \kappa_t = \kappa_c$, $\kappa_d \equiv \kappa_b = \kappa_s$, and $\kappa_\ell \equiv \kappa_\tau = \kappa_\mu$). The ranges shown for LHC and HL-LHC represent the conservative and optimistic scenarios for systematic and theory uncertainties. ILC numbers assume (e^-, e^+) polarizations of $(-0.8, 0.3)$ at 250 and 500 GeV and $(-0.8, 0.2)$ at 1000 GeV. CLIC numbers assume polarizations of $(-0.8, 0)$ for energies above 1 TeV. TLEP numbers assume unpolarized beams.*

Facility	LHC	HL-LHC	ILC500	ILC500-up	ILC1000	ILC1000-up	CLIC	TLEP (4 IPs)
$\sqrt{s}$ (GeV)	14,000	14,000	250/500	250/500	250/500/1000	250/500/1000	350/1400/3000	240/350
$\int \mathcal{L}dt$ (fb^{-1})	300/expt	3000/expt	250+500	1150+1600	250+500+1000	1150+1600+2500	500+1500+2000	10,000+2600
κ_γ	$5-7\%$	$2-5\%$	8.3%	4.4%	3.8%	2.3%	$-$/5.5/<5.5%	1.45%
κ_g	$6-8\%$	$3-5\%$	2.0%	1.1%	1.1%	0.67%	3.6/0.79/0.56%	0.79%
κ_W	$4-6\%$	$2-5\%$	0.39%	0.21%	0.21%	0.13%	1.5/0.15/0.11%	0.10%
κ_Z	$4-6\%$	$2-4\%$	0.49%	0.24%	0.44%	0.22%	0.49/0.33/0.24%	0.05%
κ_ℓ	$6-8\%$	$2-5\%$	1.9%	0.98%	1.3%	0.72%	3.5/1.4/<1.3%	0.51%
κ_d	$10-13\%$	$4-7\%$	0.93%	0.51%	0.51%	0.31%	1.7/0.32/0.19%	0.39%
κ_u	$14-15\%$	$7-10\%$	2.5%	1.3%	1.3%	0.76%	3.1/1.0/0.7%	0.69%

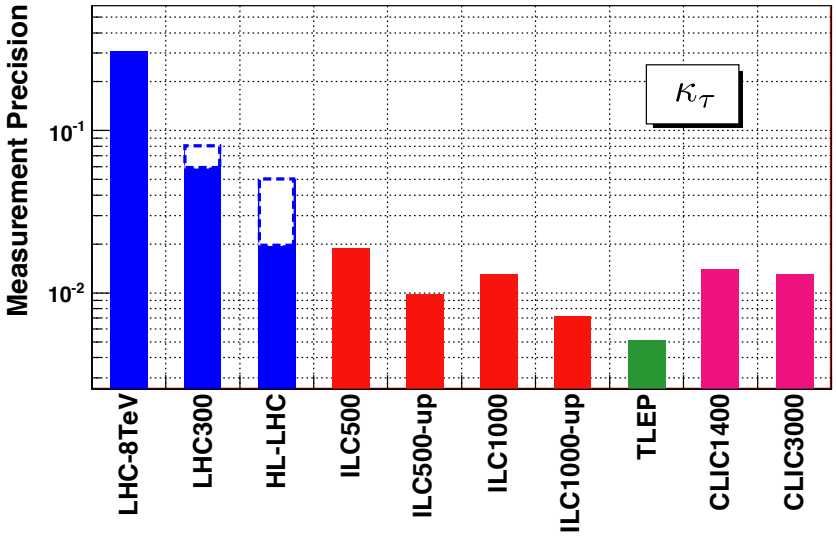

Figure 1-5. *Measurement precision on κ_τ at different facilities.*

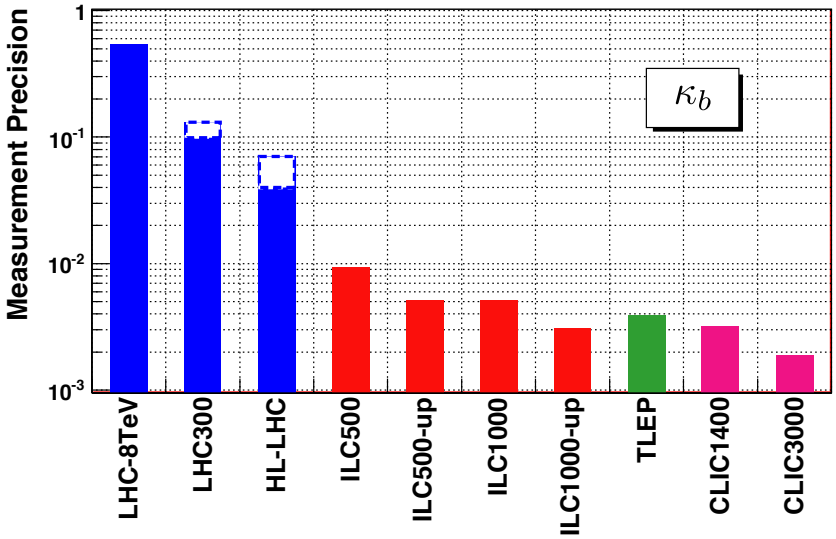

Figure 1-6. *Measurement precision on κ_b at different facilities.*

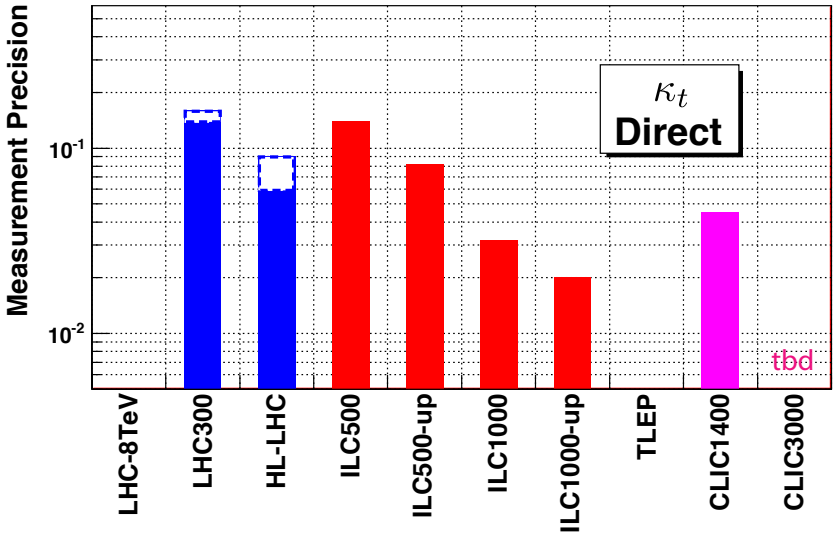

Figure 1-7. *Measurement precision on κ_t at different facilities.*

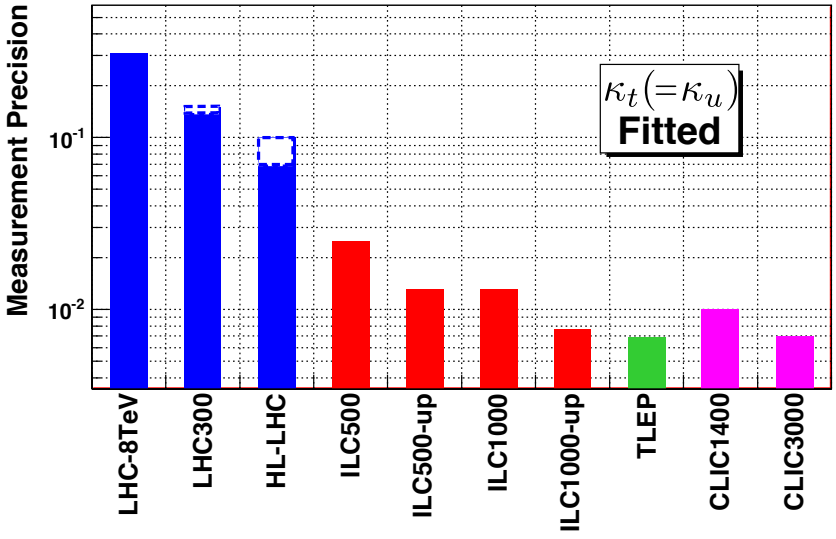

Figure 1-8. *Measurement precision on κ_u at different facilities.*

Table 1-20. *"story line" table*

Facility	HL-LHC	LHC	HL-LHC	HL-LHC
		+ ILC/ILC LumiUp	+ ILC LumiUp/TLEP+HE-LHC/TLEP+CLIC	+ HE-LHC/HE-LHC+μC
Γ_H	–			
$\mathrm{BR}_{\mathrm{inv}}$	?			
κ_γ	$2-5\%$			
κ_g	$3-5\%$			
κ_W	$2-5\%$			
κ_Z	$2-4\%$			
κ_μ	$< 10\%$			
κ_τ	$2-5\%$			
κ_c	–			
κ_b	$4-7\%$			
κ_t	$7-10\%$			

1.3 Double Higgs production and the Higgs self-coupling

Measurement of the Higgs self-coupling allows one to probe the shape of the Higgs potential. In the Standard Model, the Higgs potential can be written as (here $\langle\Phi\rangle = (0, v/\sqrt{2})^T$)

$$V = -\mu^2\Phi^\dagger\Phi + \lambda(\Phi^\dagger\Phi)^2, \tag{1.10}$$

yielding a Higgs vev and mass of

$$v = \sqrt{\mu^2/\lambda} \simeq 246 \text{ GeV}, \qquad m_h = \sqrt{2\lambda}\, v \simeq 125 \text{ GeV}. \tag{1.11}$$

The Higgs self-interaction Lagrangian, expanded about the minimum, is

$$\Delta\mathcal{L} = -\frac{1}{2}m_h^2 h^2 - \frac{g_{hhh}}{3!}h^3 - \frac{g_{hhhh}}{4!}h^4, \tag{1.12}$$

where the triple- and quartic-Higgs couplings are predicted in terms of the known Higgs mass and vev,

$$g_{hhh} = 6\lambda v = \frac{3m_h^2}{v}, \qquad g_{hhhh} = 6\lambda = \frac{3m_h^2}{v^2}. \tag{1.13}$$

The triple-Higgs coupling can be probed in double Higgs production: $gg \to hh$ at hadron colliders or $e^+e^- \to Zhh$, $\nu\bar{\nu}hh$ at lepton colliders. The main challenge is the small signal cross section. The quartic-Higgs coupling could be probed in principle through triple Higgs production, though the cross sections are too small to be detectable at any foreseen future facility.

1.3.1 Standard Model predictions for double-Higgs production

The theoretical status of double Higgs production in pp collisions has been recently summarized in Ref. [60] (Table 1-21). The most interesting process, $gg \to HH$, is currently known to next-to-leading order in QCD with a theoretical uncertainty ∼30%. This uncertainty will need to be reduced to match the anticipated experimental uncertainty at the HL-LHC and higher energy pp colliders.

All double Higgs production processes involve not only the diagram with the trilinear Higgs coupling λ, but also additional diagrams that dilute the sensitivity of the cross section measurement to λ. This dependence

Table 1-21. *Cross sections for double Higgs production in pp collisions, including the current estimate for the theoretical uncertainty from Ref. [60], for $m_H = 125$ GeV. The uncertainty on the $t\bar{t}HH$ process has not been evaluated.*

$\sqrt{s}$ (TeV)	Cross sections (fb) and theoretical uncertainties (%)				
	$gg \to HH$	$qq \to qqHH$	$q\bar{q} \to WHH$	$q\bar{q} \to ZHH$	$q\bar{q}/gg \to t\bar{t}HH$
	NLO	NLO	NNLO	NNLO	LO
14	$33.89^{+37.2\%}_{-29.8\%}$	$2.01^{+7.6\%}_{-5.1\%}$	$0.57^{+3.7\%}_{-3.3\%}$	$0.42^{+7.0\%}_{-5.5\%}$	1.02
33	$207.29^{+33.0\%}_{-26.7\%}$	$12.05^{+6.1\%}_{-4.2\%}$	$1.99^{+3.5\%}_{-3.1\%}$	$1.68^{+7.9\%}_{-6.7\%}$	7.91
100	$1417.83^{+29.7\%}_{-24.7\%}$	$79.55^{+6.2\%}_{-4.1\%}$	$8.00^{+4.2\%}_{-3.7\%}$	$8.27^{+8.4\%}_{-8.0\%}$	77.82

has been quantified for pp colliders in Ref. [60]. Because of the different kinematic dependences of the contributing diagrams, the two-Higgs invariant mass M_{HH} and the Higgs p_T distributions depend on λ. This has not yet been taken into account in LHC analyses, although an M_{HH} weighting has been used in ILC studies to increase the sensitivity to λ.

- current theoretical uncertainties for double-Higgs production at e^+e^- colliders?

1.3.2 Models that modify the hhh coupling

Beyond the Standard Model, the triple-Higgs coupling is in general modified. The size of the modification is highly model-dependent, potentially providing model-discriminating power. Estimates of the self-coupling deviation in a variety of models were recently made in Ref. [61], under the constraint that no other new physics associated with the model would be discovered by the LHC:

- Mixed-in singlets. Assuming that the mixing angle and heavy Higgs mass are such that the heavy Higgs is not detectable at the LHC, $\Delta g^{\rm max}_{hhh}/g^{\rm SM}_{hhh} \simeq -18\%$.
- Higher-dimension operators. These can come from composite Higgs models or be introduced to strengthen the electroweak phase transition to help with baryogenesis. Imposing precision electroweak constraints yields $\Delta g^{\rm max}_{hhh}/g^{\rm SM}_{hhh} \simeq \pm 20\%$.
- MSSM. The presence of the second doublet leads to mixing effects. Inclusion of top quark/squark radiative corrections is important. The largest deviations occur for low $\tan\beta$ and low M_A. For $\tan\beta \sim 5$ and $M_A \sim 200$ GeV and top squarks in the range 1–2.5 TeV, the maximum deviation is $\Delta g^{\rm max}_{hhh}/g^{\rm SM}_{hhh} \simeq -15\%$, but this number depends strongly on the other MSSM parameters and can be as low as -2%. For higher M_A the coupling deviation becomes smaller in accordance with decoupling.
- NMSSM. The additional coupling parameter λ_S from the singlet affects the scalar potential even when the singlet is decoupled. Deviations as large as $\Delta g^{\rm max}_{hhh}/g^{\rm SM}_{hhh} \simeq -25\%$ are possible for $\tan\beta \sim 7.5$, $M_A \sim 500$ GeV (outside the LHC reach) and top squark mass parameter $M_S \sim 500$ GeV, assuming that λ_S remains perturbative up to at least 10 TeV. Heavier stops lead to a smaller λ_S and the deviation becomes more similar to the MSSM.

In other models, large deviations of the triple Higgs coupling from the SM prediction can be used as characteristic signatures of the model. For example, a recent proposal [62] to improve the naturalness of SUSY models by boosting the Higgs mass using "auxiliary" scalar fields with tadpoles predicts a triple Higgs coupling much smaller than in the SM, as a consequence of the Higgs mass being generated mostly by its couplings to the auxiliary scalars. A separate study [63] of electroweak baryogenesis in a two-Higgs-doublet model or the MSSM found that successful baryogenesis resulted in deviations of the triple Higgs coupling of at least 10% or 6%, respectively.

We point out that exclusion of a coupling deviation of 20% at 95% CL requires a measurement at the 10% level; discovery of such a deviation at 5σ requires a measurement at the 4% level. This is a seriously challenging target for future LHC upgrades and proposed e^+e^- colliders.

1.3.3 Other ways to modify the double Higgs production rate

The double Higgs production cross section can also be modified by new physics separate from the triple Higgs coupling.

At the LHC, the triple Higgs coupling is measured using the $gg \to hh$ rate, which proceeds mainly through top quark triangle and box diagrams. Modification of the top quark Yukawa coupling will change the double Higgs production rate [64]. The double Higgs production rate at the LHC can also be modified by new colored particles in the loop. A color-octet scalar below 250 GeV can lead to a factor-2 enhancement of the double-Higgs production rate even for $gg \to h$ within 25% of its SM value [65]. On the other hand, vectorlike singlet or mirror quarks cause only small departures from the SM $gg \to hh$ rate once precision electroweak and $gg \to h$ constraints are imposed [66]. In all cases, the kinematic distributions of the two final-state Higgs bosons are modified with respect to the SM. Finally, in models with additional CP-even Higgs bosons (e.g., the two-Higgs-doublet models), resonant production of a heavy Higgs $gg \to H$ followed by the decay $H \to hh$ can lead to large enhancements of the double Higgs production rate at the LHC, which can be diagnosed through the resonance peak in the hh invariant mass distribution. Note that extraction of the double Higgs production cross section also relies on accurate knowledge of the Higgs decay branching ratios involved for each final state.

At an e^+e^- collider, the triple Higgs coupling is measured using the rates for $e^+e^- \to Zhh$ (dominant at 500 GeV center-of-mass energy) and $e^+e^- \to \nu\bar{\nu}hh$ (dominant at 1000 GeV or higher). These processes are also sensitive to modifications of the $VVhh$ coupling ($V = W, Z$) caused by mixing among scalars in different representations of SU(2). Such effects can potentially be separated from the triple Higgs coupling by combining measurements at different collider energies [67]. Double Higgs production at an e^+e^- collider is also susceptible to resonant contributions from heavier neutral Higgs states, such as $e^+e^- \to ZH^0$ with $H^0 \to hh$ and $e^+e^- \to hA^0$ with $A^0 \to Zh$ in two Higgs doublet models, but these processes are suppressed by $\cos^2(\beta - \alpha) \to 0$ in the decoupling limit and will also be constrained by the measurement of the SM-like Higgs couplings to W and Z bosons, $\kappa_V = \sin(\beta - \alpha)$. Such contributions can be distinguished due to their resonant kinematic structure.

1.3.4 Higgs boson self-coupling at the LHC

The self-coupling of the Higgs boson is the consequence of the electroweak symmetry breaking of the Higgs potential. Measurement of the tri-Higgs coupling will therefore allow for direct probe of the potential. This can be done through the analysis of pair production of the Higgs boson $pp \to HH + X$. At 14 TeV, the cross section is predicted to be 34 fb in the Standard Model. Table 1-22 shows the expected number of events for 3000 fb^{-1}. Statistics will be limited for final states with reasonable signal-background ratio. Combination of several final states will likely be required to achieve meaningful results.

Table 1-22. *Expected number of $pp \to HH \to XX$ events of some selected final states in a dataset of 3000 fb^{-1} at 14 TeV.*

Final state	$bb\gamma\gamma$	$bb\tau\tau$	$bbWW$	$WW\gamma\gamma$	$WW\tau\tau$	$bbbb$	$WWWW$	$\tau\tau\tau\tau$
Events	270	7,440	25,300	100	2,770	33,960	4,710	410

By far $HH \to bb\ bb$ has the highest rate. Without the signature of leptons or photons, this final state is buried under the overwhelming QCD background. Similarly $bb\ WW$ has the second highest rate, but will likely be shadowed by the $t\bar{t} \to bW\ bW$ production. There have been a number of studies [68, 60, 64] (+ ATLAS) on $bb\gamma\gamma$, $bb\tau\tau$ and $bbWW$ final states. The conclusions of these studies vary widely, ranging from over a 5σ observation [60] of the Higgs pair production to a $\sim 30\%$ precision [64] on the Higgs self-coupling parameter λ with 3000 fb^{-1}. A recent study with a generic LHC detector simulation shows that a $\sim 50\%$ precision on λ can be achieved from the $HH \to bb\gamma\gamma$ channel alone [69]. More studies are needed to firm up these estimates. For this report, a per-experiment precision of $\sim 50\%$ on λ is taken as the benchmark for HL-LHC. Combining the two experiments, a precision of 30% or better can be achieved.

Table 1-23. *Signal significance for $pp \to HH \to bb\gamma\gamma$ and percentage uncertainty on the Higgs self-coupling at future hadron colliders, from [69].*

	HL-LHC	HE-LHC	VLHC
$\sqrt{s}$ (TeV)	14	33	100
$\int \mathcal{L}dt$ (fb^{-1})	3000	3000	3000
$\sigma \cdot \mathrm{BR}(pp \to HH \to bb\gamma\gamma)$ (fb)	0.089	0.545	3.73
$S/\sqrt{B}$	2.3	6.2	15.0
λ (stat)	50%	20%	8%

Note that this extraction of the Higgs self-coupling assumes that the effective ggH coupling and the Higgs branching ratios to the final states used in the analysis are equal to their SM values.

1.3.5 Higher-energy hadron colliders

The cross section for $gg \to HH$ increases with increasing hadron collider energy due to the increase in the gluon partonic luminosity. Even though backgrounds increase with energy at a similar rate, a higher-energy pp collider like the HE-LHC (33 TeV) or VLHC (100 TeV) would improve this measurement.

Results of a fast-simulation study of double Higgs production in the $bb\gamma\gamma$ final state for pp collisions at 14, 33, and 100 TeV [69] are shown in Table 1-23 (14 TeV results are consistent with the European strategy study). $bb\gamma\gamma$ is the most important channel at 14 TeV because of large top-pair backgrounds to the $bb\tau\tau$ and $bbWW$ channels. The simulation used Delphes with ATLAS responses and assumes one detector. The resulting uncertainty on $\Delta\lambda/\lambda$ is extracted using the scaling of the double-Higgs cross section with λ [60].

1.3.6 Higgs boson self-coupling at e^+e^- Linear Colliders

At an e^+e^- linear collider, the Higgs trilinear self-coupling can be measured via the $e^+e^- \to ZHH$ and $e^+e^- \to \nu_e\bar{\nu}_e HH$ processes. The cross section for the former peaks at approximately 0.18 fb close to $\sqrt{s} = 500$ GeV; however, for this channel there are many diagrams leading to the Zhh final state that don't involve the Higgs boson self-coupling resulting in a dilution of $\Delta\lambda/\lambda \simeq 1.8 \times (\Delta\sigma_{ZHH}/\sigma_{ZHH})$. This situation improves for the W-fusion process $\nu_e\bar{\nu}_e HH$ where $\Delta\lambda/\lambda \simeq 0.85 \times (\Delta\sigma_{\nu\bar{\nu}HH}/\sigma_{\nu\bar{\nu}HH})$ at 1 TeV, but requires $\sqrt{s} \geq 1.0$ TeV for useful rates. Polarized beams can significantly increase the signal event rate, particularly for the W-fusion process. None of the proposed e^+e^- circular machines provide high enough collision energies for sufficient rates.

The most recent full simulation study [70, 49] of these two production processes including all Z decay modes as well as $HH \to bbbb$ and $HH \to bbWW^*$ final states has been carried out using the ILD detector at the ILC where event weighting depending on M_{HH} is used to enhance the contribution of the self-coupling diagram and improve on the dilutions above. Results are given in in Table 1-24.

The cross section for $\nu_e\bar{\nu}_e HH$ continues to grow with $\sqrt{s}$, and full simulation studies [51] for CLIC show increased sensitivity at higher collision energies of $\sqrt{s} = 1.4$ TeV and $\sqrt{s} = 3.0$ TeV as shown in Table 1-24.

Table 1-24. *Estimated experimental percentage uncertainties on the double Higgs production cross sections and Higgs self-coupling parameter λ from e^+e^- linear colliders. The expected precision on λ assumes that the contributions to the production cross section from other diagrams take their Standard Model values. ILC numbers include bbbb and bbWW* final states and assume (e^-, e^+) polarizations of $(-0.8, 0.3)$ at 500 GeV and $(-0.8, 0.2)$ at 1000 GeV. ILC500-up is the luminosity upgrade at 500 GeV, not including any 1000 GeV running. ILC1000-up is the luminosity upgrade including running at both 500 and 1000 GeV. CLIC numbers include only the bbbb final state. The two numbers for each CLIC energy are without/with 80% electron beam polarization. ‡ILC luminosity upgrade assumes an extended running period on top of the low luminosity program and cannot be directly compared to CLIC numbers without accounting for the additional running period.*

	ILC500	ILC500-up	ILC1000	ILC1000-up	CLIC1400	CLIC3000
$\sqrt{s}$ (GeV)	500	500	500/1000	500/1000	1400	3000
$\int \mathcal{L}dt$ (fb^{-1})	500	1600‡	500+1000	1600+2500‡	1500	+2000
$P(e^-, e^+)$	$(-0.8, 0.3)$	$(-0.8, 0.3)$	$(-0.8, 0.3/0.2)$	$(-0.8, 0.3/0.2)$	$(0, 0)/(-0.8, 0)$	$(0, 0)/(-0.8, 0)$
$\sigma(ZHH)$	42.7%	?	42.7%	23.7%	–	–
$\sigma(\nu\bar{\nu}HH)$	–	–	26.3%	16.7%	?	?
λ	83%	46%	21%	13%	28/21%	16/10%

1.3.7 Photon collider

Higgs pairs can be produced at a photon collider via off-shell s-channel Higgs production, $\gamma\gamma \to H^* \to HH$. The process was studied in Ref. [71] for an ILC-based photon collider running for 5 years, leading to 80 raw $\gamma\gamma \to HH$ events. Jet clustering presents a major challenge for signal survival leading to a sensitivity of only about 1σ.

1.3.8 Muon collider

Double Higgs production at a muon collider can proceed via s-channel off-shell Higgs production, $\mu^+\mu^- \to h^* \to HH$. However, the cross section for this non-resonant process is very small, of order 1.5 ab at the optimum energy of ~ 275 GeV, providing less than one signal event in 500 fb^{-1} before branching ratios and selection efficiencies are folded in.

1.3.9 Summary

Expected precisions on the triple Higgs coupling measurement, assuming that all other Higgs couplings are SM-like and that no other new physics contributes to double-Higgs production, are summarized in Table 1-25.

Table 1-25. *Expected per-experiment precision on the triple-Higgs boson coupling. ILC numbers include bbbb and bbWW* final states and assume (e^-, e^+) polarizations of $(-0.8, 0.3)$ at 500 GeV and $(-0.8, 0.2)$ at 1000 GeV. ILC500-up is the luminosity upgrade at 500 GeV, not including any 1000 GeV running. ILC1000-up is the luminosity upgrade with a total of 1600 fb^{-1} at 500 GeV and 2500 fb^{-1} at 1000 GeV. CLIC numbers include only the bbbb final state and assume 80% electron beam polarization. HE-LHC and VLHC numbers are from fast simulation [69] and include only the bbγγ final state. ‡ILC luminosity upgrade assumes an extended running period on top of the low luminosity program and cannot be directly compared to CLIC numbers without accounting for the additional running period.*

	HL-LHC	ILC500	ILC500-up	ILC1000	ILC1000-up	CLIC1400	CLIC3000	HE-LHC	VLHC
$\sqrt{s}$ (GeV)	14000	500	500	500/1000	500/1000	1400	3000	33,000	100,000
$\int \mathcal{L}dt$ (fb^{-1})	3000/expt	500	1600‡	500+1000	1600+2500‡	1500	+2000	3000	3000
λ	50%	83%	46%	21%	13%	21%	10%	20%	8%

1.4 Study of *CP*-mixture and spin

The discovery of the new boson with the mass around 126 GeV at the LHC [72, 73] opens a way for experimental studies of its properties such as spin, parity, and couplings to the Standard Model particles. We split such studies into two groups

- tests of discrete spin/parity hypotheses of the new particle(s);
- identification and measurement of various types of tensor couplings for a given spin assignment, and the search for *CP* violation is among the primary goals of this study.

There is a potential connection between the baryogenesis and *CP* violation in the Higgs sector and the measurements in the Higgs sector directly may be complementary to the measurements in the EDMs [74]. The interesting level of *CP*-odd state admixture angle θ is $|\sin\theta| < 0.1$.

We note that several facts about the Higgs-like boson spin, parity, and its couplings have already been established. Indeed, we know that

- the new boson should have integer spin since it decays to two integer-spin particles [72, 73];
- the new boson cannot have spin one because it decays to two on-shell photons [75, 76]
- the spin-one assignment is also strongly disfavored by the measurement of angular distributions in the decay to two Z bosons [77, 78, 79, 80, 81];
- under the assumption of minimal coupling to vector bosons or fermions, the new boson is unlikely to be a spin-two particle [77, 78, 79, 80, 81];
- the spin-zero, negative parity hypothesis is strongly disfavored [77, 78, 79, 80, 81];

The general amplitudes that describe the interaction of the spin-zero, spin-one, and spin-two boson can be found in the literature [82, 83]. In particular, the minimal coupling gravity-like coupling of spin-2 boson to gauge boson is chosen as a benchmark spin model in the study. For *CP*-mixing studies of parity and couplings of the spin-zero Higgs-like boson may employ either effective Lagrangians or generic parameterizations of

scattering amplitudes. For the coupling to the gauge bosons, such as ZZ, WW, $Z\gamma$, $\gamma\gamma$, or gg, the scattering amplitude can be written as

$$A(X_{J=0} \to VV) = v^{-1}\left(a_1 m_V^2 \epsilon_1^* \epsilon_2^* + a_2 f_{\mu\nu}^{*(1)} f^{*(2),\mu\nu} + a_3 f_{\mu\nu}^{*(1)} \tilde{f}^{*(2),\mu\nu}\right) . \tag{1.14}$$

The SM Higgs coupling at tree level (to ZZ and WW) is described by the a_1 term, while the a_2 term appears in the loop-induced processes, such as $Z\gamma$, $\gamma\gamma$, or gg. The a_3 term corresponds to the pseudoscalar. The general scattering amplitude that describes the interaction of the Higgs-like boson with the fermions, such as $\tau^+\tau^-$, $\mu^+\mu^-$, $b\bar{b}$, and $t\bar{t}$, can be written as

$$A(X_{J=0} \to f\bar{f}) = \frac{m_f}{v}\bar{u}_2\left(b_1 + b_2\gamma_5\right)u_1 , \tag{1.15}$$

The two constants b_1 and b_2 correspond to the scalar and pseudoscalar couplings. It is important to note that each set of constants, such as a_1, a_2, a_3, is generally independent between different coupling types (ZZ, $\gamma\gamma$, etc) and does not correspond directly to the mixture of the original state (relative strength of those could be rather different from the actual mixture).

CP violation in the Higgs sector could be revealed if both *CP*-odd and *CP*-even contributions are detected. It has already been established that the *CP*-even contribution dominates at least in the HZZ coupling [77, 78, 79, 80, 81]. Therefore, measuring or setting the limit on the *CP*-odd contribution is a target of the study. Four independent real numbers describe bosonic process and two real numbers describe fermionic process provided that the overall rate is treated separately and one overall complex phase is not measurable. For a vector boson coupling, we can represent the four independent parameters by two fractions of the corresponding cross-sections (f_{a2} and f_{a3}) and two phases (ϕ_{a2} and ϕ_{a3}). In particular, the fraction of *CP*-odd contribution is defined as (f_{a3} in the case of boson couplings)

$$f_{CP} = \frac{|a_3|^2\sigma_3}{\sum |a_i|^2\sigma_i} \tag{1.16}$$

We note that σ_i is the effective cross-section of the Higgs boson decay process corresponding to $a_i = 1, a_{j\neq i} = 0$. For example, for the $H \to ZZ$ decay, $\sigma_3/\sigma_1 \simeq 0.160$.

In Table 1-26 we summarize expected precision of spin and *CP*-mixture measurements at different facilities and running conditions. For various effective couplings, precision is quoted on *CP*-odd cross-section fraction, such as f_{CP} defined above. For the measurement precision we estimate that 10% admixture [74] of pseudoscalar in a Higgs state is a reasonable target. The scalar Higgs couplings to massive vector bosons (ZZH and WWH) are at tree level, while pseudoscalar coupling is expected to be suppressed by a loop. Therefore, the 10% admixture of a pseudoscalar in a Higgs state would translate to a significantly suppressed *CP*-odd contribution, with f_{CP} smaller than 10^{-5} in the $H \to ZZ$ and WW decays. On the other hand, in the fermion couplings and vector boson couplings suppressed by a loop for both scalar and pseudoscalar (ggH, $\gamma\gamma H$, $Z\gamma H$), both couplings could be of comparable size, and the target precision on f_{CP} is 10^{-2} or better.

With the current luminosity of about 25 fb^{-1} at 7 and 8 TeV, both ATLAS and CMS experiments expect more than 2σ separation between the minimal spin-2 model and SM Higgs boson [77, 78, 79, 80, 81]. This translates to close to 10σ separation at high luminosity.

LHC expectation in *CP* studies comes from dedicated analysis of the $H \to ZZ^*$ decay [32, 77, 78, 79, 81] by CMS and ATLAS collaborations and as well as individual studies [84, 85]. The CMS experiment quotes 0.40 expected error on f_{CP} with present statsitics [78, 79], which translates to ± 0.07 and ± 0.02 at 300 fb^{-1} and 3000 fb^{-1}, respectively [32]. These results scale well with luminosity and cross-section and match those reported in dedicated studies.

The VBF production at LHC [82] offers a complementary way to measure *CP* mixture in the VVH coupling. Using kinematic correlations of jets in the VBF topology with the full matrix element technique, a fraction of about 0.05 (015) of *CP*-odd cross-section contribution can be measured at 3000 (300) fb^{-1} on LHC [85]. Given different relative cross-sections of the VBF production of the scalar and pseudoscalar components, these translate to the equivalent value of f_{CP} defined for decay in Eq. (1.16) of 0.0005 (0.003). The issue of increasing pileup was not addressed in detail in this study. However, reduced precision with increased thresholds for jets checked in this study would be easily compensated by considering additional final states of the Higgs boson, since this study depends only a particular production mechanism and not the final states.

The spin study at e^+e^- is based on TESLA TDR studies [39]. A threshold scan with a luminosity of 20 fb^{-1} at three centre-of-mass energies (215, 222, and 240 GeV for $m_H = 120$ GeV) is sufficient to distinguish the spin-1 and spin-2 hypotheses at 4σ level. This study has been recently updated [86] to include the Higgs boson mass and luminosity and energy scenarios. The typical probability for most exotic scenarios is smaller than 10^{-6}. This study is based on assumption of 250 fb^{-1} at 250 GeV and 20 fb^{-1} at each of three energy points below.

Table 1-26. *List of expected precision of spin and CP-mixture measurements. Spin significance is quoted for one representative model of minimal coupling KK graviton $J^P = 2^+_m$. For various effective couplings, precision is quoted on CP-odd cross-section fraction, such as f_{a3} defined for $H \to ZZ^*$. Target precision is estimated to be $< 10^{-5}$ for the modes with pseudoscalar coupling expected to be suppressed by a loop (ZZH and WWH), while it is estimated to be $< 10^{-2}$ for fermion couplings and vector boson couplings suppressed by a loop for both scalar and pseudoscalar (ggH, $\gamma\gamma H$, $Z\gamma H$). Numerical values are given where reliable estimates are provided, ✓ mark indicates that some studies are done and measurement is in principle possible or feasibility of such a measurement could be considered.*

Collider	pp	pp	e^+e^-	e^+e^-	e^+e^-	e^+e^-	$\gamma\gamma$	$\mu^+\mu^-$	target
E (GeV)	14,000	14,000	250	350	500	1,000	126	126	(theory)
$\mathcal{L}$ (fb^{-1})	300	3,000	250	350	500	1,000	250		
spin-2^+_m	$\sim 10\sigma$	$\gg 10\sigma$	$>10\sigma$	$>10\sigma$	$>10\sigma$	$>10\sigma$			$>5\sigma$
ZZH	$0.07^\dagger$	$0.02^\dagger$	$7{\cdot}10^{-4}$	$1.1{\cdot}10^{-4}$	$4{\cdot}10^{-5}$	$7{\cdot}10^{-6}$	✓	✓	$< 10^{-5}$
WWH	$3{\cdot}10^{-3\ddagger}$	$5{\cdot}10^{-4\ddagger}$	✓	✓	✓	✓	✓	✓	$< 10^{-5}$
ggH	✓	✓	–	–	–	–	–	–	$< 10^{-2}$
$\gamma\gamma H$	–	–	–	–	–	–	0.06	–	$< 10^{-2}$
$Z\gamma H$	–	✓	–	–	–	–	–	–	$< 10^{-2}$
$\tau\tau H$	–	–	0.01	0.01	0.02	0.06	✓	✓	$< 10^{-2}$
ttH	✓	✓	–	–	0.29	0.08	–	–	$< 10^{-2}$
$\mu\mu H$	–	–	–	–	–	–	–	✓	$< 10^{-2}$

† estimated in $H \to ZZ^*$ decay mode

‡ estimated in $V^*V^* \to H$ (VBF) production mode

The *CP* mixture study at an e^+e^- collider was shown based on 500 fb^{-1} at the centre-of-mass energy of 350 GeV and $m_H = 120$ GeV [39]. A recent study [84,85] compares expected performance of an e^+e^- collider and LHC. Precision on *CP*-odd cross-section fraction of 0.036 (0.044) is obtained at 250 GeV (500 GeV) scenarios. However, these fractions correspond to different f_{CP} values in the $H \to ZZ$ decay, due to different relative

strength of *CP*-odd and *CP*-even couplings. The corresponding precision on f_{CP} is 0.0007(0.00004) [84, 85], assuming that no strong momentum dependence of couplings happens at these energies.

A promising channel to study *CP* violation is the decay $H \to \tau^+\tau^-$. Spin correlations are possible to use in the τ decay. For example, pion is preferably emitted in the direction of the τ spin in the τ rest frame. These studies are performed in the clean e^+e^- environment, while it is extremely difficult in the proton collisions. Several studies have been performed, in the hadronic final states [87], decays $\tau \to \rho\nu$ [88], and all final states [89,90]. All studies agree on a similar precision of about 5° for the typical scenarios in Table 1-26, where the study in Ref. [87] includes full simulation of signal and background. The above estimate translates to approximately 0.01 precision on f_{CP}. The precision becomes somewhat worse with increased collider energy due to reduced ZH production cross-section, and this technique relies on the knowledge of the Z vertex.

A study of *CP*-odd contribution in the ttH coupling has been studied in the context of ILC [91]. Cross-section dependence on the coupling has been employed and an uncertainty of 0.08 (0.29) at 1000 (500) GeV center-of-mass energy has been estimated. A beam polarization of (+0.2,-0.8) and (+0.3,-0.8) is assumed at 1000 and 500 GeV, respectively. These estimates further improve to 0.05 (0.16) for the luminosity upgrade of the ILC.

Beam polarization in the photon and muon colliders would be essential for *CP* measurements in the $\gamma\gamma H$ and $\mu\mu H$ couplings. Three parameters $\mathcal{A}_1, \mathcal{A}_2, \mathcal{A}_3$ sensitive to *CP* violation have been defined in the context of the photon collider [92, 93, 94]. The $\mathcal{A}_1$ parameter can be measured as an asymmetry in the Higgs boson production cross-section between the A_{++} and A_{--} circular polarizations of the beams. This asymmetry is the easiest to measure, but it is proportional to $\mathcal{I}m(a_2 a_3^*)$ and is zero when in Eq. (1.14) a_2 and a_3 are real, as expected for the two loop-induced couplings with heavier particles in the loops. A more interesting parameter

$$\mathcal{A}_3 = \frac{|A_\parallel|^2 - |A_\perp|^2}{|A_\parallel|^2 + |A_\perp|^2} = \frac{2\mathcal{R}e\,(A^*_{--}A_{++})}{|A_{++}|^2 + |A_{--}|^2} = \frac{|a_2|^2 - |a_3|^2}{|a_2|^2 + |a_3|^2} = (1 - 2f_{CP}) \tag{1.17}$$

can be measured as an asymmetry between two configurations with the linear polarization of the photon beams, one with parallel and the other with orthogonal polarizations. In Ref. [95] careful simulation of the process has been performed. The degree of linear polarization at the maximum energies is 60% for the electron beam $E_0 \approx 110$ GeV and the laser wavelength $\lambda \approx 1\,\mu m$. The expected uncertainty on $\mathcal{A}_3$ is 0.11 for $2.5 \cdot 10^{34} \times 10^7 = 250$ fb^{-1} integrated luminosity. This translates to the f_{CP} uncertainty of 0.06. The *CP* mixture study at a photon collider was also shown based on a sample of 50,000 raw $\gamma\gamma \to h$ events assuming 80% circular polarization of both electron beams [58]. This study corresponds to the $\mathcal{A}_1$ asymmetry measurement, with expected precision on $\mathcal{A}_1$ of about 1%.

On the muon collider, the *CP* quantum numbers of the states can be determined if the muon beams can be transversely polarized. The cross section for production of a resonance [96] depends on P_T (P_L), the degree of transverse (longitudinal) polarization of each of the beams and ζ is the angle of the μ^+ transverse polarization relative to that of the μ^- measured using the direction of the μ^- momentum as the z axis. In particular, muon beams polarized in the same transverse direction selects out the *CP*-even state, while muon beams polarized in opposite transverse directions (i.e., with spins $+1/2$ and $-1/2$ along one transverse direction) selects out the *CP*-odd state.

Several other measurements are possible on pp, e^+e^-, photon, and muon colliders, which are left to future feasibility studies. In Table 1-26 we summarize various couplings where *CP* measurements are possible.

1.5 Mass and Total Width Measurements

A broadening of the total width of the Higgs boson relative to Standard Model predictions is the clearest, model-independent discovery mode for new physics. The experimental challenge is to make a model-independent measurement of the total width that reaches the level of the theoretical uncertainty on this quantity in the Standard Model. The total width of the Standard Model Higgs boson is predicted to be approximately 4 MeV for a boson with a mass of 125 GeV. The Standard Model decay modes to $b\bar{b}$, W^+W^-, $\tau^+\tau^-$, gg, $c\bar{c}$, and ZZ account in total for over 99% of the total width. The Higgs to $b\bar{b}$ branching fraction at roughly 58%±3% is the single largest contribution to the theoretical uncertainty on the total width at this time. With further measurement improvements on α_s, precision couplings, and QCD lattice calculations, the Standard Model prediction on the total width will achieve approximately X% accuracy. The experimental measurement of the Higgs to $b\bar{b}$ branching fraction in ZH production to sub-percent accuracy will reduce the uncertainty on the Higgs total width prediction to 1%.

There are three proposed techniques to access the total width of the Higgs boson: interferometry in $gg(\rightarrow H) \rightarrow \gamma\gamma$ or $gg(\rightarrow H) \rightarrow ZZ$, measuring a partial width via a cross section and the corresponding branching fraction, and a direct lineshape scan.

The mass of the Higgs boson provides an important self-consistency test of the electroweak Standard Model at the quantum level: radiative corrections involving the Higgs boson contribute to the SM prediction for the W mass. At current precisions, the electroweak fit indirectly predicts $m_H = 94^{+29}_{-24}$ GeV (1σ range) [97]. Foreseeable improvements of m_t to 0.1 GeV, M_W to 5–6 MeV, and $\sin^2\theta^{lept}_{\rm eff}$ to 1.3×10^{-5} achievable at ILC/GigaZ option would tighten this constraint to $\delta m_H \approx \pm 10$ GeV [97]. A discrepancy between the SM prediction for m_H extracted from the precision electroweak fit and the directly-measured mass would constitute clear evidence for new physics. The current sub-GeV uncertainty in the Higgs mass from the LHC experiments [25, 26] is already much better than the precision needed to make this test.

The Higgs mass uncertainty also feeds into the uncertainty on the Higgs couplings to SM fermions and gauge bosons through the kinematic dependence of the Higgs branching ratios. A 100 MeV uncertainty in m_H corresponds to a 0.5% uncertainty in the ratio of couplings κ_b/κ_W.

The mass of the Higgs boson is the most sensitive parameter in determining whether the electroweak vacuum is stable. A vacuum-to-vacuum decay of the Higgs vacuum expectation value from the electroweak scale to the Planck scale would cause a massive increase in the relative strength of the gravitational forces on elementary particles and cause catastrophic changes to the large-scale structures in the universe. Assuming only the SM up to the Planck scale, the Higgs mass needed for vacuum stability is given by [61, 98]

$$m_H > 129.4 \text{ GeV} + 1.4 \text{ GeV} \left(\frac{m_t - 173.2 \text{ GeV}}{0.7 \text{ GeV}} \right) - 0.5 \text{ GeV} \left(\frac{\alpha_s(M_Z) - 0.1184}{0.0007} \right) \pm 1 \text{ GeV}, \qquad (1.18)$$

where the last ±1 GeV is the theoretical uncertainty coming mainly from the low-energy matching scale for the quartic coupling in the Higgs potential. The top quark mass uncertainty plays an important role. To match a Higgs mass uncertainty of $\delta m_H \sim 150$ MeV, the top mass uncertainty must be below 100 MeV, comparable to the expected uncertainty from an e^+e^- threshold scan.

Another use of the Higgs mass is to test parameter relations in theories beyond the SM, such as the MSSM, in which the Higgs mass is predicted in terms of the Z boson mass, $\tan\beta$, M_A, and radiative corrections coming mainly from top-quark and top-squark loops. The latter depend strongly on m_t, leading to an uncertainty in the predicted Higgs mass of order 100 MeV for $\delta m_t \sim 100$ MeV [61]. The usefulness of a Higgs mass measurement at the 100 MeV level or below thus depends on a precision measurement of the top quark mass.

Results from different facilities below are summarized in Table 1-27.

1.5.1 Hadron colliders

The Higgs boson mass can be measured directly from the $H \to \gamma\gamma$ and $H \to ZZ^* \to 4\ell$ decays at the LHC. Based on the dataset taken during the 2011-2012 running of a combined luminosity of ~ 25 fb^{-1} at 7 and 8 TeV, ATLAS and CMS have measured the mass to be $125.5 \pm 0.2(\text{stat})^{+0.5}_{-0.6}(\text{syst})$ GeV [25] and $125.7 \pm 0.3(\text{stat}) \pm 0.3(\text{syst})$ GeV [26] respectively, with a poor-man's average of 0.25 GeV uncertainty from the statistics and 0.45 GeV for the systematics.

The statistical uncertainty on the mass of the current measurement is already smaller (or comparable) than the systematic uncertainty. With the expected $\times 2.5$ increase in Higgs cross section from 8 TeV to 14 TeV, the statistical uncertainty is expected to reduce to $\sim$ 50 MeV and $\sim$ 15 MeV with 300 and 3000 fb^{-1} at 14 TeV. Thus the precision of the future measurement will likely be dominated by systematics. The largest contribution is the knowledge of the energy/momentum scale of photons, electrons and muons, which should improve with increasing statistics. If one makes the optimistic assumption that that the systematics also scales with statistics, the expected systematic uncertainty is $\sim$ 70 MeV and $\sim$ 25 MeV at 300 and 3000 fb^{-1}. At this precision, theoretical issues such as the interference between the $H \to \gamma\gamma$ resonance and the continuum will need to be taken into account. However, the $H \to ZZ^* \to 4\ell$ decay is not expected to suffer from such interference, in particular the $H \to ZZ^* \to 4\mu$ decay should be free of the limitations from many of experimental and systematic uncertainties. These arguments suggest that a precision of $\sim$ 100 MeV and $\sim$ 50 MeV per experiment on the Higgs mass should be achievable at the LHC with 300 and 3000 fb^{-1}.

Both ATLAS and CMS have studied Higgs mass precisions in their technical design reports [99, 100] (Fig. 19-45 of the ATLAS report and Fig. 10.37 of CMS report). ATLAS estimates that a relative precision of 0.07% is achievable with 300 fb^{-1} while CMS projects a statistical uncertainty of 0.1% with 30 fb^{-1}, both for $m_H = 125$ GeV. These results are consistent with the estimates above.

The most direct method of measuring of the Higgs width is to fit the mass distributions of the observed $H \to \gamma\gamma$ and $H \to ZZ^* \to 4\ell$ resonances. However, since the experimental mass resolutions are much larger than the expected SM Higgs width, this method is not expected to be sensitive to Γ_H^{SM} (≈ 4.2 MeV). Indeed the expected upper bound on Γ_H from the CMS $H \to \gamma\gamma$ analysis of the 7 and 8 TeV datasets is 5.9 GeV Ref[CMS-PAS-HIG-13-016], or $1400 \times \Gamma_H^{SM}$. With the assumption that the bound scales with the number of Higgs candidates and combining with the $H \to ZZ^* \to 4\ell$ analysis, an upper limit of $\sim$ 200 MeV should be possible with 3000 fb^{-1}, corresponds to $\sim 50 \times \Gamma_H^{SM}$.

New theoretical developments by S. Martin, L. Dixon, and Y. Li [101, 102, 103] open the possibility to significantly improve the sensitivity using the Higgs mass measurement in the $\gamma\gamma$ channel. Interference between $gg \to H \to \gamma\gamma$ and the continuum $gg \to \gamma\gamma$ background cause a shift in the reconstructed Higgs mass in the $\gamma\gamma$ final state of about -70 MeV [103], which grows with increasing Higgs total width. A comparison of the Higgs mass determination in $ZZ \to 4\mu$ and $\gamma\gamma$ should thus be able to make an $\mathcal{O}(100\%)$ measurement of the Higgs total width, though no study of the possible future precision has been done. Because the sign of the mass shift depends on the sign of $\kappa_g\kappa_\gamma$, this measurement also has the potential to determine the relative sign of these two loop-induced couplings.

Another approach was very recently proposed in Ref. [104] using interference between $gg \to ZZ$ and $gg \to h \to ZZ$ for ZZ invariant masses above the pair-production threshold. Based on the current LHC data for the ZZ production cross section, Ref. [104] estimates a bound $\Gamma_H \leq 20$–$38\,\Gamma_H^{\text{SM}}$ at 95% CL, depending on the 4ℓ invariant mass range studied and assuming that $\kappa_g\kappa_Z$ has the same sign as in the SM. The ultimate precision of this method will be limited by the uncertainty on the ZZ cross section; taking an optimistic 3% ultimate precision on the cross section would yield a Higgs width bound of $\Gamma_H \leq 5$–$10\,\Gamma_H^{\text{SM}}$ at 95% CL.

More stringent limit on Γ_H can be set from the coupling fit with the assumption of $\kappa_W, \kappa_Z \leq 1$. From Table 1-14, an upper bound of $\sim \Gamma_H^{SM}/(1 - \text{BR}_{\text{BSM}}) \approx 1.12 \times \Gamma_H^{SM}$ can be obtained with 3000 fb^{-1}.

Assuming only SM productions and decays, the total Higgs width can be measured with a $5-8\%$ precision at the HL-LHC.

1.5.2 e^+e^- colliders

Using the process $e^+e^- \to ZH$ with $Z \to \mu^+\mu^-$ and $Z \to e^+e^-$, plus a measurement of the beamstrahlung energy distribution, a precision measurement of the Higgs mass can be made from the shape and distribution of the invariant mass recoiling against the reconstructed Z [46, 45, 51, 105]. Indeed, the specification of required momentum resolution in the linear collider detector designs, particularly for muons, is optimized on the precision of the mass measurement.

To address the total Higgs width, as described in Sec. 1.2, at lower energies of $\sqrt{s} \sim 250$ GeV this involves a measurement of the total production cross section in $e^+e^- \to ZH$, independent of branching ratios, which can be done using the recoil mass technique. The partial width $\Gamma(H \to ZZ)$ is directly proportional to the cross section, and from a measurement of the complementary branching fraction $\mathrm{BR}(H \to ZZ)$, a totally model-independent total Higgs width can be extracted: $\Gamma_H = \Gamma(H \to ZZ)/\mathrm{BR}(H \to ZZ)$. At higher energies, a measurement of the cross section for the WW-fusion process $e^+e^- \to \nu_e\bar{\nu}_e H$ along with $\mathrm{BR}(H \to WW^*)$ provides a further improvement on the extracted width.

1.5.3 Muon collider

A direct lineshape scan of the Higgs boson in s-channel production will achieve sub-MeV precision on the mass. This precision is unmatched using any other known technique. The beam spread and beam energy resolution at a muon collider is good enough to resolve the SM Higgs width of ~ 4 MeV directly through a line scan with a precision of 4.3%.

The Higgs total width is predicted to be 3×10^{-5} of the resonance center-of-mass energy. Therefore, a beam energy scan will be needed to locate the central value of the Higgs resonance. Input on the mass value from previous measurements will be important to reduce the scan range. The muon collider proposal [59] envisions measuring the Higgs mass, total width, and production rates in the bb, WW^* and $\tau\tau$ final states with a 5-point energy scan centered on the Higgs resonance at $\sqrt{s} \sim 126$ GeV, with scan point separation of 4.07 MeV. The run scenario assumes 1 Snowmass year (10^7 s) at 1.7×10^{31} cm^{-2}s^{-1} plus 5 Snowmass years at 8.0×10^{31} cm^{-2}s^{-1} and a beam energy resolution of $R = 4 \times 10^{-5}$. Achievable precisions on the Higgs mass and width are $\Delta m_H = 0.06$ MeV and $\Delta\Gamma_H = 0.18$ MeV $= 4.3\%$.

1.5.4 Summary

A summary of the Higgs mass and width measurement capabilities for the facilities is given in Table 1-27.

Table 1-27. *Summary of the Higgs mass and total width measurement precisions of various facilities.* ‡*ILC luminosity upgrade assumes an extended running period on top of the low luminosity program and cannot be directly compared to TLEP and CLIC numbers without accounting for the additional running period. The ILC assumes 0.1% theory uncertainties.*

Facility	LHC	HL-LHC	ILC500	ILC1000	ILC1000-up	CLIC	TLEP (4 IP)	μC
$\sqrt{s}$ (GeV)	14,000	14,000	250/500	250/500/1000	250/500/1000	350/1400/3000	240/350	126
$\int \mathcal{L}dt$ (fb^{-1})	300	3000	250+500	250+500+1000	1150+1600+2500‡	500+1500+2000	10,000+2600	
m_H (MeV)	100	50	35	35	?	33	7	0.06
Γ_H	–	–	5.9%	5.6%	2.7%	8.4%	0.6%	4.3%

1.6 pMSSM

The pMSSM is a phenomenological version of the MSSM with 19 input parameters. The parameters are constrained to be consistent with current experimental limits. A scan over input parameters looks at regions in parameter space which can be excluded by measurements of the Higgs couplings. For example, a measurement of κ_τ (with the central value given by the Standard Model prediction) would exclude 32.4% of the parameter space at the HL-LHC, and 78% of the parameter space at the ILC500. Combining all Higgs coupling measurements, the HL-LHC would exclude 34% of the pMSSM parameter space, while ILC500 excludes 99.7% of the parameter space [106].

1.7 Direct searches for BSM Higgs bosons H^0, A^0, $H^\pm$

1.7.1 Theory

Many well-motivated extensions of the SM contain a second Higgs doublet, including the MSSM. Including a second doublet introduces an additional four scalar degrees of freedom beyond the SM-like Higgs boson h. These are commonly denoted H^0 (CP-even neutral), A^0 (CP-odd neutral), and $H^\pm$ (charged Higgs pair). If CP is violated in the Higgs sector, the three neutral states (including h) can be CP mixtures.

Because electroweak symmetry breaking is shared between the two doublets, the couplings of the additional scalars depend on the couplings of the discovered SM-like Higgs boson h. Here we assume that h is nearly SM-like and the new scalars are heavier than h. The two Higgs doublets can be written as Φ_1 and Φ_2 with

$$\Phi_j = \begin{pmatrix} \phi_j^+ \\ \phi_j^0 \end{pmatrix} = \begin{pmatrix} \phi_j^+ \\ (v_j + \phi_j^{0,r} + i\phi_j^{0,i})/\sqrt{2} \end{pmatrix}, \tag{1.19}$$

where v_1 and v_2 are the vacuum expectation values of the two doublets normalized according to $v_1^2 + v_2^2 = v_{\rm SM}^2 \simeq 246$ GeV. Their ratio is a free parameter $\tan\beta \equiv v_2/v_1$. The second free parameter α is the mixing angle in the h–H^0 sector. The "mismatch" between the two mixing angles, $\cos(\beta-\alpha)$, controls how SM-like the Higgs h is.

In the *decoupling limit*, $M_{H^0} \simeq M_{A^0} \simeq M_{H^\pm} \gg M_Z$, the properties of h approach those of the SM Higgs boson. This limit occurs in the MSSM when $M_A \gg M_Z$. It also occurs in more general two Higgs doublet models (2HDMs) when the scalar quartic couplings are not allowed to become too large. In this limit, discovery of the heavy Higgs particles becomes difficult because of kinematic suppression of cross sections.

1.7.2 LHC constraints and projections

The heavy Higgs bosons H^0, A^0, and $H^\pm$ have been searched for at the LHC in the context of the MSSM, as well as a more general search for H^0 in WW and ZZ final states in a two-Higgs-doublet model.

H^0 and A^0 are produced through gluon fusion as well as $b\bar{b}$ fusion at large $\tan\beta$. Production cross sections are rescaled from the SM gluon-fusion calculations of the LHC Higgs Cross Sections Working Group [6] and the $b\bar{b}$ fusion code `bbh@nnlo` [107]. $b\bar{b}$ fusion dominates the production cross section for moderate to large $\tan\beta$, leading to highest sensitivity at large $\tan\beta$. Decay branching ratios are calculated assuming the MSSM m_h^{max} scenario with $M_{\text{SUSY}} = 1$ TeV. This implies that the H^0 and A^0 signals are both present and their mass splitting is fixed point-by-point in the parameter space.

From a search for the $\tau\tau$ final state using 17 fb^{-1} at 7 and 8 TeV, CMS excludes M_A values below 800 GeV for $\tan\beta = 50$, falling to 250 GeV for $\tan\beta = 5$ (no exclusion is made for $\tan\beta < 5$) [108]. Searches in the $\mu\mu$ final state have much better mass resolution but are currently less sensitive due to the smaller branching ratio.

LHC searches for heavy Higgs states in a generic 2HDM are also underway. ATLAS searched for $H^0 \to WW$ in the context of Type-I and -II 2HDMs for various $\tan\beta$ values as a function of the mixing angle α, and excludes ranges of α for M_{H^0} as high as 250 GeV (13 fb^{-1} at 8 TeV) [109].

The direct search for heavy Higgs bosons at the LHC in the MSSM excludes regions in the $\tan\beta$-M_A plane. At relatively low M_A, the region at high $\tan\beta$ is excluded by searches for $A \to \tau^+\tau^-$, while at smaller $\tan\beta$ and small M_A the exclusion results from the heavier H decaying to ZZ and W^+W^-. With 25 fb^{-1}, Ref. [16] estimates that for all values of $\tan\beta$ the region below about $M_A \sim 200$ GeV can be excluded. The location of this wedge is increased to ~ 380 GeV with 300 fb^{-1} [whitepaper by Ian Lewis].

If A^0 and $H^\pm$ are not too heavy, they will be pair produced at LHC via the electroweak processes $pp \to H^\pm A^0$, H^+H^-, with the decays $A^0 \to bb$ and $H^\pm \to \tau\nu$ dominating in large parts of the MSSM and 2HDM parameter space. The cross section depends only on the particle masses. A recent parton-level study [110] estimated that both processes should be discoverable at the 14 TeV LHC with less than 20 fb^{-1} if $M_A \sim 95$–130 GeV and, in fact, could already be discoverable in the current 8 TeV LHC data-set.

At low $\tan\beta$, signals of interest are decays of A^0/H^0 to charginos or neutralinos (this depends strongly on SUSY model spectrum assumptions). Also decays $A^0 \to Zh$, $H^0 \to hh$, $H^0/A^0 \to \gamma\gamma$, and $H^0 \to WW$ are of interest.

1.7.3 Projections for e^+e^- machines

At an e^+e^- collider, the cross section for $e^+e^- \to Z^* \to H^0Z$ is suppressed by $\cos^2(\beta-\alpha)$ compared to the cross section for a SM Higgs with the same mass as H^0. In the decoupling limit, the associated production cross section for $e^+e^- \to Z^* \to H^0A^0$, which is proportional to $\sin^2(\beta-\alpha)$, is maximal, but requires associated production of two heavy particles, limiting the kinematic reach to half the collider center-of-mass energy (similarly for $e^+e^- \to H^+H^-$). Charged Higgs pair production, $e^+e^- \to H^+H^-$, is a pure gauge process and hence also unsuppressed. With sufficient luminosity, the discovery reach for these states at an e^+e^- collider is thus close to the kinematic limit,

$$M_{H^+} < \sqrt{s}/2, \qquad M_{H^0} + M_{A^0} < \sqrt{s}. \tag{1.20}$$

Because the mass splitting between H^0 and A^0 is typically small in the decoupling region, the reach for either of them is roughly $\sqrt{s}/2$ [111].

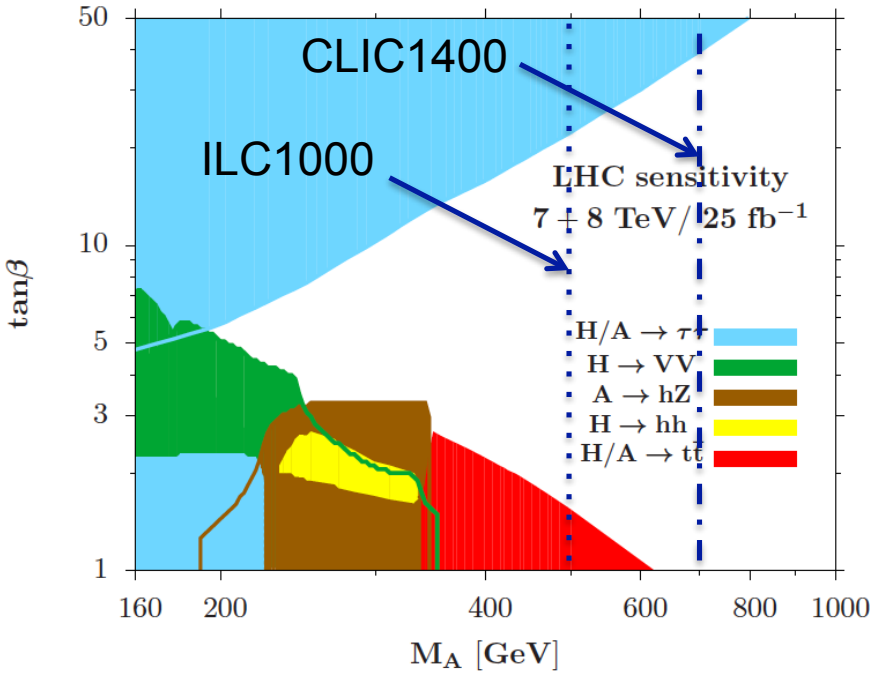

Figure 1-9. *MSSM Higgs sector search reach in the m_A–$\tan\beta$ plane for e^+e^- colliders compared to the expected LHC 7+8 TeV upper limits (95% C.L.).*

1.7.4 Resonant production at a muon collider

The neutral heavy Higgs bosons H^0 and A^0 can be produced as s-channel resonances in $\mu^+\mu^-$ or $\gamma\gamma$ collisions. They can also be pair produced via electroweak processes as at e^+e^- machines.

If the heavy Higgs bosons H^0 and A^0 are not very light, resonant production at a muon collider may be the best opportunity to study their properties in detail. This was studied in Ref. [112] for the "Natural Supersymmetry" benchmark point of Ref. [113], which has $M_{A^0} \simeq M_{H^0} \simeq 1.55$ TeV and $\tan\beta = 23$. The mass difference between A^0 and H^0 is about 10 GeV and their decay widths are around 20 GeV.

The parton-level analysis [112] was based on a center-of-mass energy scan over a 200 GeV range centered at 1550 GeV in 100 steps, collecting a total of 500 fb^{-1}. Signal and background cross sections in the $b\bar{b}$ and $\tau\tau$ final states were computed using PYTHIA6 modified to include a Gaussian beam energy spread of 0.1%. The overlapping lineshapes were then fitted with two Breit-Wigners in the $b\bar{b}$ final state (a single Breit-Wigner is ruled out at high confidence) allowing extraction of the masses to ± 0.5 GeV, the widths to $\sim 3.5\%$, and the peak $\sigma \times \mathrm{BR}(b\bar{b})$ to 9% for the two states. The $\tau\tau$ channel can then be used to measure $\mathrm{BR}(\tau\tau)/\mathrm{BR}(b\bar{b})$ with an uncertainty of about 10%. As a bonus, decays of H^0 and A^0 to charginos or neutralinos may provide the largest sample of the heavier ones of these particles, whose direct production cross sections can be quite small at lepton colliders [112].

The *CP* quantum numbers of the states can be determined if the muon beams can be transversely polarized, see Sec. 1.4 for details. This would allow identification of the two resonances as A^0 and H^0 as well as probing for *CP*-violating mixing between the states. Similar techniques are possible at a photon collider.

1.7.5 Resonant production at a photon collider

The neutral heavy Higgs bosons H^0 and A^0 can be produced as s-channel resonances in high-energy $\gamma\gamma$ collisions. Such a high-energy photon collider could be realized as an option at a high-energy e^+e^- collider such as ILC or CLIC. The photon collider offers the following features:

- High mass reach, $M_{H^0,A^0} \simeq \sqrt{s_{\gamma\gamma}}$.
- Selective production of CP-even or CP-odd states through photon beam polarization.
- Capability to measure ratios of couplings by taking ratios of rates into different final states.
- Sensitivity to the loop-induced $H^0\gamma\gamma$ and $A^0\gamma\gamma$ couplings through the production cross section, measured in the form $\sigma \times$ BR.

1.8 Conclusions

A precision Higgs physics program is compelling because the Standard Model precisely predicts all Higgs boson couplings and properties with no free parameters, now that the Higgs mass is known. Any deviation from these predictions therefore represents clear evidence for new physics. The current outlook on high-$p_{\rm T}$ physics from 8 TeV LHC operation and the first measurements of the boson at 126 GeV indicate that the standard for discovering new physics in the Higgs sector beyond the 300fb^{-1}, 14 TeV LHC program requires an order of magnitude improvement in the measurement of Higgs couplings and properties. This requirement translates to percent-level precisions in the leading couplings of the Higgs to matter. The primary and perhaps most fundamental conclusion of this report is that a precision Higgs program requires a combined program of high statistics production of the 126 GeV boson in an lepton collider environment and a comprehensive evaluation of the fundamental parameters that enter the theory-experimental comparisons.

The following list are bulleted conclusions, highlighting the main outcomes of this report.

- The Higgs boson, a new state of matter, has been discovered at the LHC. Understanding the properties of this new state is of fundamental importance and deserves further investigation in the form of a precision experimental program. Any deviation in the predicted properties of the Higgs boson is a strong, unabiguious signature for new physics. Comparisons for different Higgs physics programs are provided in terms of the measurement precision on the mass, total width, spin, couplings, CP mixtures, and the searches for multiple Higgs bosons.
- Full exploitation of LHC and HL-LHC Higgs measurements will require improvements in theoretical calculations of the gluon fusion Higgs production cross section, both inclusive and with jet vetoes. To match sub-percent experimental uncertainties on Higgs partial widths from Higgs factories will require consistent inclusion of higher order electroweak corrections to Higgs decays, as well as an improvement of the bottom quark mass determination to below ± 0.01 GeV.
- LHC is the place to study Higgs boson in the next decade. The expected precision of Higgs couplings to fermions and vector bosons, assuming only SM decay modes, are estimated to be 4–15% for 300 fb^{-1} and 2-10% for 3000 fb^{-1} at 14 TeV. Better precisions can be achieved for some coupling ratios.
- Given sufficient integrated luminosity, all Higgs boson decays, including invisible or exotic final states, are accessible in the ZH production mode at an e^+e^- collider through the model-independent recoil mass technique.

- Precision tests of Higgs boson couplings to one-percent will require complementary precision programs. Proposed Higgs factories such as linear or circular e^+e^- colliders and potentially a muon collider will be able to achieve these precisions for many of the absolute couplings, and in a model-independent way.

- HL-LHC can measure the Higgs boson mass with a precision of ∼50 MeV per experiment, however has limited sensitivity to the Higgs decay total width even with SM assumptions. Higgs factories such as ILC, CLIC, or TLEP will achieve a mass precision of about 35 MeV and measure Higgs decay width up to ∼1.3% in precision. Through a line-shape scan, a muon collider can measure the total width directly to 4.3% and the mass to sub-MeV precision.

- Direct ttH coupling measurements can be done at LHC, ILC, CLIC and muon colliders. The expected precisions are 7–10% at HL-LHC per experiment, 2–3% at ILC with luminosity upgrade and 3% at CLIC. A high energy muon collider is expected to have the comparable precision as CLIC per experiment.

- Higgs self-coupling is difficult to measure at any of these facilities. A 50% measurement per experiment is expected from HL-LHC and 13% from linear e^+e^- colliders at 1 TeV. Improvement would need higher collision energies, with CLIC achieving 10% at 3 TeV and VLHC achieving 8% at 100 TeV.

- The spin of the 126 GeV boson will be constrained by the LHC. A limited parameter space of spin-two couplings may be left to be constrained by the data from the future facilities.

- Potential *CP*-odd fraction in $H \to ZZ^*$ cross-section (f_{CP}) will be measured by LHC to a few percent precision, with further improvement in VBF production. The e^+e^- machines can measure this to a greater precision in the $ee \to ZH$. *CP* admixture in fermion couplings is not expected to suffer from loop suppression and can be studied in $H \to \tau\tau$ decay and ttH production, leading to about 1% precision on f_{CP} in $\tau\tau H$ coupling at an e^+e^- machine. The photon and muon colliders are unique in their capability to probe *CP* violation directly with polarized beams.

- There are strong theoretical arguments for physics beyond the Standard Model. The LHC and CLIC have the highest discovery potential for heavy Higgs bosons as predicted by many Standard Model extensions. At the LHC, the mass reach can be 1 TeV or higher with 3000 fb^{-1} at 14 TeV, but is strongly model dependent. The mass reach is generally limited to less than half the collision energy for e^+e^- colliders and potentially up to the collision energy for a muon collider through s-channel processes.

We have also arrived to the following facility comparison:

- LHC at 14 TeV with 300 fb^{-1} of data is essential to firmly establish the five major production mechanisms of a Higgs boson (ggH, VBF, WH, ZH, $t\bar{t}H$) and the main bosonic and fermionic decay modes ($b\bar{b}$, WW^*, $\tau^+\tau^-$, ZZ^*, $\gamma\gamma$). This will lead to about a factor of 3–5 improvement in the most precise measurements compared to the 8 TeV run of LHC. This will also lead to about 100 MeV precision on the Higgs boson mass and the measurement of the boson spin.

- HL-LHC provides unique capabilities to measure rare statisically limited SM decay modes such as $\mu^+\mu^-$, $\gamma\gamma$, and $Z\gamma$ and make the first measurements of the Higgs self-coupling. The high luminosity program increases the precision on the couplings compared to the LHC with 300 fb^{-1} by roughly a factor of 2–3 and has a high discovery potential for heavy Higgs bosons.

- TeV-scale e^+e^- linear colliders (ILC and CLIC) offer the full menu of measurements of the 126 GeV Higgs boson with better precision than the LHC, though their mass reach for heavy Higgs bosons are generally weaker than high-energy pp colliders, except for CLIC running at 3 TeV. The two linear colliders have different capabilities – the ILC can run on the Z peak while CLIC has a higher mass reach and better precision in Higgs self-coupling measurement when operating at 3 TeV.
- TLEP offers the best precisions for most of the Higgs coupling measurements because of its projected integrated luminosity and multiple detectors. This program also includes high luminosity operation at the Z peak and top threshold. There is no sensitivity to ttH and HHH couplings at these center-of-mass energies.
- A higher energy pp collider such as a 33 TeV(HE-LHC) or 100 TeV(VLHC) hadron collider provides high sensitivity to the Higgs self-coupling as well as the highest discovery potential for heavy Higgs bosons.
- A TeV-scale muon collider should have similar physics capabilities as the ILC and CLIC with potentially higher energy reach, but this needs to be demonstrated with more complete studies. The muon collider also has the potential for resonant production of heavy Higgs bosons. CP measurements are possible if a beam polarization option is included.
- A $\gamma\gamma$ collider is able to study CP mixture and violation in the Higgs sector with polarized photon beams. It can improve the precision of the effective $\gamma\gamma H$ coupling measurement through s-channel production.

References

[1] M. Aicheler *et al.*, Report No. CERN-2012-007. SLAC-R-985. KEK-Report-2012-1. PSI-12-01. JAI-2012-001, 2012 (unpublished).

[2] T. Behnke *et al.*, *The International Linear Collider Technical Design Report - Volume 1: Executive Summary*, (2013), 1306.6327.

[3] Luminosity upgrade parameters at 250 GeV come from private communication from ILC accelerator physicists, Marc Ross and Nick Walker.

[4] M. Koratzinos *et al.*, *TLEP: A High-Performance Circular e+e- Collider to Study the Higgs Boson*, (2013), 1305.6498.

[5] A. Denner, S. Heinemeyer, I. Puljak, D. Rebuzzi, and M. Spira, *Standard Model Higgs-Boson Branching Ratios with Uncertainties*, Eur.Phys.J. **C71**, 1753 (2011), 1107.5909.

[6] The LHC Higgs Cross Section Working Group, S. Heinemeyer *et al.*, *Handbook of LHC Higgs Cross Sections: 3. Higgs Properties*, (2013), 1307.1347.

[7] LHC Higgs Cross Section Working Group, S. Dittmaier, C. Mariotti, G. Passarino, and R. Tanaka (Eds.), *Handbook of LHC Higgs Cross Sections: 2. Differential Distributions*, CERN-2012-002 (CERN, Geneva, 2012), 1201.3084.

[8] Particle Data Group, J. Beringer *et al.*, *Review of Particle Physics (RPP)*, Phys.Rev. **D86**, 010001 (2012).

[9] C. McNeile, C. Davies, E. Follana, K. Hornbostel, and G. Lepage, *High-Precision c and b Masses, and QCD Coupling from Current-Current Correlators in Lattice and Continuum QCD*, Phys.Rev. **D82**, 034512 (2010), 1004.4285.

[10] K. Chetyrkin *et al.*, *Charm and Bottom Quark Masses: An Update*, Phys.Rev. **D80**, 074010 (2009), 0907.2110.

[11] R. S. Gupta, H. Rzehak, and J. D. Wells, *How well do we need to measure Higgs boson couplings?*, Phys.Rev. **D86**, 095001 (2012), 1206.3560.

[12] G. M. Pruna and T. Robens, *The Higgs Singlet extension parameter space in the light of the LHC discovery*, (2013), 1303.1150.

[13] N. Craig, J. Galloway, and S. Thomas, *Searching for Signs of the Second Higgs Doublet*, (2013), 1305.2424.

[14] C.-Y. Chen, S. Dawson, and M. Sher, *Heavy Higgs Searches and Constraints on Two Higgs Doublet Models*, (2013), 1305.1624.

[15] M. S. Carena, H. E. Haber, H. E. Logan, and S. Mrenna, *Distinguishing a MSSM Higgs boson from the SM Higgs boson at a linear collider*, Phys.Rev. **D65**, 055005 (2002), hep-ph/0106116.

[16] A. Djouadi and J. Quevillon, *The MSSM Higgs sector at a high M_{SUSY}: reopening the low tanβ regime and heavy Higgs searches*, (2013), 1304.1787.

[17] D. Carmi, A. Falkowski, E. Kuflik, and T. Volansky, *Interpreting LHC Higgs Results from Natural New Physics Perspective*, JHEP **1207**, 136 (2012), 1202.3144.

[18] N. Arkani-Hamed, K. Blum, R. T. D'Agnolo, and J. Fan, *2:1 for Naturalness at the LHC?*, JHEP **1301**, 149 (2013), 1207.4482.

[19] M. Carena, S. Gori, N. R. Shah, C. E. M. Wagner, and L.-T. Wang, *Light Stops, Light Staus and the 125 GeV Higgs*, (2013), 1303.4414.

[20] LHC Higgs Cross Section Working Group, S. Dittmaier *et al.*, *Handbook of LHC Higgs Cross Sections: 1. Inclusive Observables*, (2011), 1101.0593.

[21] R. D. Ball, M. Bonvini, S. Forte, S. Marzani, and G. Ridolfi, *Higgs production in gluon fusion beyond NNLO*, (2013), 1303.3590.

[22] R. Boughezal, F. Caola, K. Melnikov, F. Petriello, and M. Schulze, *Higgs boson production in association with a jet at next-to-next-to-leading order in perturbative QCD*, JHEP **1306**, 072 (2013), 1302.6216.

[23] L. H. C. S. W. Group *et al.*, *LHC HXSWG interim recommendations to explore the coupling structure of a Higgs-like particle*, (2012), 1209.0040.

[24] CDF Collaboration, D0 Collaboration, T. Aaltonen *et al.*, *Higgs Boson Studies at the Tevatron*, (2013), 1303.6346.

[25] ATLAS Collaboration, G. Aad *et al.*, *Measurements of Higgs boson production and couplings in diboson final states with the ATLAS detector at the LHC*, (2013), 1307.1427.

[26] CMS Collaboration, *Combination of standard model Higgs boson searches and measurements of the properties of the new boson with a mass near 125 GeV*, (2013).

[27] ATLAS Collaboration, *Search for a Standard Model Higgs boson in $H \to \mu\mu$ decays with the ATLAS detector.*, (2013).

[28] ATLAS Collaboration, *Search for the Standard Model Higgs boson in the $H \to Z\gamma$ decay mode with pp collisions at $\sqrt{s} = 7$ and 8 TeV*, (2013).

[29] CMS Collaboration, S. Chatrchyan *et al.*, *Search for a Higgs boson decaying into a Z and a photon in pp collisions at $\sqrt{s} = 7$ and 8 TeV*, (2013), 1307.5515.

[30] ATLAS Collaboration, *Search for invisible decays of a Higgs boson produced in association with a Z boson in ATLAS*, (2013).

[31] ATLAS Collaboration, *Physics at a High-Luminosity LHC with ATLAS*, (2013), 1307.7292.

[32] CMS Collaboration, *Projected Performance of an Upgraded CMS Detector at the LHC and HL-LHC: Contribution to the Snowmass Process*, (2013), 1307.7135.

[33] P. Onyisi, R. Kehoe, V. Rodriguez, and Y. Ilchenko, *Analysis of t tbar H Events at sqrt(s)=14 TeV with $H \to WW$*, (2013), 1307.7280.

[34] G. T. Bodwin, F. Petriello, S. Stoynev, and M. Velasco, *Higgs boson decays to quarkonia and the Hccbar coupling*, (2013), 1306.5770.

[35] H. Murayama and M. E. Peskin, *Physics opportunities of e^+e^- linear colliders*, Ann. Rev. Nucl. Part. Sci. **46**, 533 (1996), hep-ex/9606003.

[36] ECFA/DESY LC Physics Working Group, E. Accomando *et al.*, *Physics with e^+e^- linear colliders*, Phys.Rept. **299**, 1 (1998), hep-ph/9705442.

[37] S. Dawson and M. Oreglia, *Physics opportunities with a TeV linear collider*, Ann.Rev.Nucl.Part.Sci. **54**, 269 (2004), hep-ph/0403015.

[38] American Linear Collider Working Group, T. Abe *et al.*, *Linear Collider Physics Resource Book for Snowmass 2001 - Part 2: Higgs and Supersymmetry Studies*, (2001), hep-ex/0106056.

[39] ECFA/DESY LC Physics Working Group, J. Aguilar-Saavedra *et al.*, *TESLA: The Superconducting electron positron linear collider with an integrated x-ray laser laboratory. Technical design report. Part 3. Physics at an e+ e- linear collider*, (2001), hep-ph/0106315.

[40] ACFA Linear Collider Working Group, K. Abe *et al.*, *Particle physics experiments at JLC*, (2001), hep-ph/0109166.

[41] ILC, G. Aarons *et al.*, *International Linear Collider Reference Design Report Volume 2: Physics at the ILC*, (2007), 0709.1893.

[42] J. E. Brau *et al.*, *The Physics Case for an e+e- Linear Collider*, (2012), 1210.0202.

[43] H. Baer *et al.*, *The International Linear Collider Technical Design Report - Volume 2: Physics*, (2013), 1306.6352.

[44] A. Blondel *et al.*, *LEP3: A High Luminosity e^+e^- Collider to study the Higgs Boson*, arXiv:1208.0504v2, ESPP contribution 138, 2012.

[45] P. Azzi *et al.*, *Prospective studies for LEP3 with the CMS detector*, arXiv:1208.1662, ESPP contribution 171, 2012.

[46] T. Abe *et al.*, *The International Large Detector: Letter of Intent*, ILD Concept Group, arXiv:1006.3396 [hep-ex], 2010.

[47] H. Aihara *et al.*, *SiD Letter of Intent*, SiD Concept Group, arXiv:0911.0006 [physics.ins-det], 2009.

[48] T. Behnke *et al.*, *The International Linear Collider Technical Design Report – Volume 4: Detectors*, arXiv:1306.6329, 2013.

[49] D. Asner *et al.*, *ILC Higgs White Paper*, Snowmass-xxx, 2013.

[50] H. Baer *et al.*, *The International Linear Collider Technical Design Report – Volume 2: Physics*, arXiv:1306.6352, 2013.

[51] CLIC Detector and Physics Study Collaboration, H. Abramowicz *et al.*, *Physics at the CLIC e^+e^- Linear Collider – Input to the Snowmass process 2013*, (2013), 1307.5288.

[52] P. Janot *et al.*, *First Look at the Physics case of TLEP*, Snowmass-xxx White Paper, 2013.

[53] P. Janot *et al.*, *TLEP Physics Case: First Look*, talk presented at Snowmass Energy Frontier Workshop, Seattle, June 30 – July 3, 2013.

[54] C. Farrell and A. H. Hoang, *Next-to-leading-logarithmic QCD corrections to the cross-section sigma(e+ e- to t anti-t H) at 500-GeV*, Phys.Rev. **D74**, 014008 (2006), hep-ph/0604166.

[55] R. Yonamine *et al.*, *Measuring the top Yukawa coupling at the ILC at $\sqrt{s} = 500$ GeV*, Phys.Rev. **D84**, 014033 (2011), 1104.5132.

[56] D. Asner *et al.*, *Higgs physics with a gamma gamma collider based on CLIC I*, Eur.Phys.J. **C28**, 27 (2003), hep-ex/0111056.

[57] S. Bogacz *et al.*, *SAPPHiRE: a Small Gamma-Gamma Higgs Factory*, (2012), 1208.2827.

[58] W. Chou, G. Mourou, N. Solyak, T. Tajima, and M. Velasco, *HFiTT - Higgs Factory in Tevatron Tunnel*, (2013), 1305.5202.

[59] D. B. Cline *et al.*, *Muon Collider Higgs Factory for Snowmass 2013*, (2013).

[60] J. Baglio *et al.*, *The measurement of the Higgs self-coupling at the LHC: theoretical status*, JHEP **1304**, 151 (2013), 1212.5581.

[61] R. S. Gupta, H. Rzehak, and J. D. Wells, *How well do we need to measure the Higgs boson mass and self-coupling?*, (2013), 1305.6397.

[62] J. Galloway, M. A. Luty, Y. Tsai, and Y. Zhao, *Induced Electroweak Symmetry Breaking and Supersymmetric Naturalness*, (2013), 1306.6354.

[63] S. Kanemura, Y. Okada, and E. Senaha, *Electroweak baryogenesis and quantum corrections to the triple Higgs boson coupling*, Phys.Lett. **B606**, 361 (2005), hep-ph/0411354.

[64] F. Goertz, A. Papaefstathiou, L. L. Yang, and J. Zurita, *Higgs Boson self-coupling measurements using ratios of cross sections*, JHEP **1306**, 016 (2013), 1301.3492.

[65] G. D. Kribs and A. Martin, *Enhanced di-Higgs Production through Light Colored Scalars*, Phys.Rev. **D86**, 095023 (2012), 1207.4496.

[66] S. Dawson, E. Furlan, and I. Lewis, *Unravelling an extended quark sector through multiple Higgs production?*, Phys.Rev. **D87**, 014007 (2013), 1210.6663.

[67] R. Killick, K. Kumar, and H. E. Logan, *Learning what the Higgs is mixed with*, (2013), 1305.7236.

[68] M. J. Dolan, C. Englert, and M. Spannowsky, *Higgs self-coupling measurements at the LHC*, JHEP **1210**, 112 (2012), 1206.5001.

[69] W. Yao, *Studies of $HH \to bb\gamma\gamma$ for Higgs self-coupling measurements at the future hadron colliders*, (2013).

[70] J. Tian, *Study of Higgs Self-coupling at the ILC based on full detector simulation at $\sqrt{s} = 500$ and 1000 GeV*, LC-REP-2013-003, 2013.

[71] S.-i. Kawada *et al.*, *A feasibility study of the measurement of Higgs pair creation at a Photon Linear Collider*, Phys.Rev. **D85**, 113009 (2012), 1205.5292.

[72] ATLAS, G. Aad *et al.*, *Observation of a new particle in the search for the Standard Model Higgs boson with the ATLAS detector at the LHC*, Phys. Lett. B **716**, 1 (2012), 1207.7214.

[73] CMS, S. Chatrchyan *et al.*, *Observation of a new boson at a mass of 125 GeV with the CMS experiment at the LHC*, Phys. Lett. B **716**, 30 (2012), 1207.7235.

[74] J. Shu and Y. Zhang, *Impact of a CP Violating Higgs: from LHC to Baryogenesis*, (2013), 1304.0773.

[75] L. D. Landau, *On the angular momentum of a two-photon system*, Dokl. Akad. Nauk **60**, 207 (1948).

[76] C. N. Yang, *Selection Rules for the Dematerialization of a Particle into Two Photons*, Phys. Rev. **77**, 242 (1950).

[77] CMS Collaboration, S. Chatrchyan *et al.*, *On the mass and spin-parity of the Higgs boson candidate via its decays to Z boson pairs*, Phys.Rev.Lett. **110**, 081803 (2013), 1212.6639.

[78] CMS Collaboration, *Updated results on the new boson discovered in the search for the standard model Higgs boson in the ZZ to 4 leptons channel in pp collisions at sqrt(s) = 7 and 8 TeV*, (2012).

[79] CMS Collaboration, *Properties of the Higgs-like boson in the decay H to ZZ to 4l in pp collisions at sqrt s =7 and 8 TeV*, (2013).

[80] CMS Collaboration, *Evidence for a particle decaying to W+W- in the fully leptonic final state in a standard model Higgs boson search in pp collisions at the LHC*, (2013).

[81] ATLAS Collaboration, G. Aad *et al.*, *Evidence for the spin-0 nature of the Higgs boson using ATLAS data*, (2013), 1307.1432.

[82] E. Accomando *et al.*, *Workshop on CP Studies and Non-Standard Higgs Physics*, (2006), hep-ph/0608079.

[83] Y. Gao *et al.*, *Spin determination of single-produced resonances at hadron colliders*, Phys. Rev. D **81**, 075022 (2010), 1001.3396.

[84] A. Whitbeck *et al.*, *Higgs CP: Comparison of LHC and e^+e^- collider*, talk at High Energy Frontier Workshop on Future of Particle Physics, Seattle, July 2013.

[85] Y. Gao *et al.*, *HVV CP Update: Comparison of LHC and e^+e^- collider*, talk at HEP Community Summer Study, Minneapolis, August 2013.

[86] K. Kruger, *e^+e^- summary and updated on Higgs spin and CP*, talk at High Energy Frontier Workshop on Future of Particle Physics, Seattle, July 2013.

[87] M. Reinhard and H. Videau, talk at Geneve 10, 2010.

[88] K. Desch, A. Imhof, Z. Was, and M. Worek, *Probing the CP nature of the Higgs boson at linear colliders with tau spin correlations: The Case of mixed scalar - pseudoscalar couplings*, Phys.Lett. **B579**, 157 (2004), hep-ph/0307331.

[89] S. Berge, *Determination of the CP parity of Higgs boson in their tau decay channel at the ILC*, talk at High Energy Frontier Workshop on Future of Particle Physics, Seattle, July 2013.

[90] S. Berge, W. Bernreuther, and H. Spiesberger, *Determination of the CP parity of Higgs bosons in their tau decay channels at the ILC*, (2012), 1208.1507.

[91] K. Fujii *et al.*, *CP mixture with ttH at ILC*, talk at HEP Community Summer Study, Minneapolis, August 2013.

[92] B. Grzadkowski and J. Gunion, *Using back scattered laser beams to detect CP violation in the neutral Higgs sector*, Phys.Lett. **B294**, 361 (1992), hep-ph/9206262.

[93] M. Kramer, J. H. Kuhn, M. Stong, and P. Zerwas, *Prospects of measuring the parity of Higgs particles*, Z.Phys. **C64**, 21 (1994), hep-ph/9404280.

[94] J. Gunion and J. Kelly, *Determining the CP eigenvalues of the neutral Higgs bosons of the minimal supersymmetric model in gamma gamma collisions*, Phys.Lett. **B333**, 110 (1994), hep-ph/9404343.

[95] D. M. Asner, J. B. Gronberg, and J. F. Gunion, *Detecting and studying Higgs bosons at a photon-photon collider*, Phys.Rev. **D67**, 035009 (2003), hep-ph/0110320.

[96] B. Grzadkowski, J. F. Gunion, and J. Pliszka, *How valuable is polarization at a muon collider? A Test case: Determining the CP nature of a Higgs boson*, Nucl.Phys. **B583**, 49 (2000), hep-ph/0003091.

[97] A. Freitas *et al.*, *Exploring Quantum Physics at the ILC*, (2013), 1307.3962.

[98] G. Degrassi *et al.*, *Higgs mass and vacuum stability in the Standard Model at NNLO*, JHEP **1208**, 098 (2012), 1205.6497.

[99] and CERN, *ATLAS: Detector and physics performance technical design report. Volume 2*, (1999).

[100] CMS Collaboration, G. Bayatian *et al.*, *CMS technical design report, volume II: Physics performance*, J.Phys. **G34**, 995 (2007).

[101] S. P. Martin, *Shift in the LHC Higgs diphoton mass peak from interference with background*, Phys.Rev. **D86**, 073016 (2012), 1208.1533.

[102] S. P. Martin, *Interference of Higgs diphoton signal and background in production with a jet at the LHC*, (2013), 1303.3342.

[103] L. J. Dixon and Y. Li, *Bounding the Higgs Boson Width Through Interferometry*, (2013), 1305.3854.

[104] F. Caola and K. Melnikov, *Constraining the Higgs boson width with ZZ production at the LHC*, (2013), 1307.4935.

[105] ILD Design Study Group, H. Li *et al.*, *HZ Recoil Mass and Cross Section Analysis in ILD*, (2012), 1202.1439.

[106] M. Cahill-Rowley, J. Hewett, A. Ismail, and T. Rizzo, *Constraints on Higgs Properties and SUSY Partners in the pMSSM*, (2013), 1308.0297.

[107] R. V. Harlander and W. B. Kilgore, *Higgs boson production in bottom quark fusion at next-to-next-to leading order*, Phys.Rev. **D68**, 013001 (2003), hep-ph/0304035.

[108] CMS Collaboration, *Higgs to tau tau (MSSM) (HCP)*, (2012).

[109] ATLAS Collaboration, *Search for Higgs bosons in Two-Higgs-Doublet models in the $H \to WW \to e\nu\mu\nu$ channel with the ATLAS detector*, (2013).

[110] N. D. Christensen, T. Han, and T. Li, *Pair Production of MSSM Higgs Bosons in the Non-decoupling Region at the LHC*, Phys.Rev. **D86**, 074003 (2012), 1206.5816.

[111] L. Linssen, A. Miyamoto, M. Stanitzki, and H. Weerts, editors, *Physics and Detectors at CLIC: CLIC Conceptual Design Report* (, 2012), ANL-HEP-TR-12-01, CERN-2012-003, DESY 12-008, KEK Report 2011-7, arXiv:1202.5940.

[112] E. Eichten and A. Martin, *The Muon Collider as a H/A factory*, (2013), 1306.2609.

[113] H. Baer and J. List, *Post LHC7 SUSY benchmark points for ILC physics*, (2012), 1205.6929.